# Control Methodologies for Powered Orthoses for People with Ambulatory Disabilities

By

Andrés Martínez Guerra

Dissertation

Submitted to the Faculty of the

Graduate School of Vanderbilt University

in partial fulfillment of the requirements

for the degree of

DOCTOR OF PHILOSOPHY

in

Mechanical Engineering

August 9, 2019

Nashville, Tennessee

Approved:

Michael Goldfarb, Ph.D.

Karl Zelik, Ph.D.

Eric Barth, Ph.D.,

Kevin Galloway, Ph.D.

Ryan Farris, Ph.D.

# DEDICATION

To my parents, Joaquin and Lorena,
and my sister, Laura,
for their unconditional support

# ACKNOWLEDGEMENTS

This dissertation, along with all my work in the Center for Rehabilitation Engineering and Assistive Technology (CREATE), formerly Center for Intelligent Mechatronics (CIM), is a contribution to a larger research effort undertaken by Michael Goldfarb, doctoral students that preceded me, and others that will come after me. As a result, I must acknowledge Michael Goldfarb as the creative and intellectual leader of this research project. His research projects, funding, and business partnership with Parker Hannifin collectively led to my place as a graduate student in his lab. I am grateful to have taken a part in his legacy.

Several researchers and engineers have played important roles in this work and my graduate studies. I would like to thank Drs. Karl Zelik, Eric Barth, Kevin Galloway, and Ryan Farris for serving as members of my dissertation committee. I am thankful for their input to making my research project the best it could have been during my time at Vanderbilt University.

A special thank you to Brian Lawson, Don Truex, and Christina Durrough. Brian was instrumental in welcoming me to the lab, guiding me through the transition to graduate school, and advising me on my project. Similarly, Don was always willing to listen to my questions and provide guidance to solutions. Lastly, thank you to Chrissy, for your valuable feedback regarding my research progression and for helping with subject recruitment.

My work would not have been possible without the support of the Human Motion and Control team at Parker Hannifin. They developed the iterations of the Indego exoskeleton I worked with, and provided hardware and software support when needed.

Thank you to all the members of CREATE (and formerly CIM) I got to spend time in the lab with. You made my experience in the lab the most enjoyable years in school I've had.

Above all, I must thank my parents, Lorena and Joaquin, and my sister, Laura, for playing significant roles in my life and throughout my studies. I would not be where I am today without your unconditional love and support.

# PREFACE

The research presented in this document was completed as part of my doctoral work in mechanical engineering. My work focuses on developing controllers to use in powered orthoses for people with ambulatory disabilities. As such, my work was limited to developing controllers and testing for direct effect (i.e., when the user is wearing the device) on the users' gait kinematics. My work did not investigate indirect effects (i.e., effects that linger after using and removing the device). Indirect effects of orthotic interventions are beyond the scope a mechanical engineering dissertation. Further, measuring indirect effects is beyond the expertise of the Center for Rehabilitation and Assistive Technology at Vanderbilt University. Thus, all assessments detailed in this document measure the direct effects of control methodologies for orthotic interventions in a limited number of subjects. The controllers developed in this research were not tested for indirect effect. Results from this research only indicate improvements due to direct effect. This dissertation does not claim to improve users' gait symmetry and kinematics after wearing the device, despite the possibility of doing so.

TABLE OF CONTENTS

Page

LIST OF FIGURES

LIST OF TABLES

# LIST OF DEFINITIONS AND ACRONYMS

Terms used to categorize individuals with ambulatory disabilities:

- **Non-ambulatory individual:** individuals who have no motor function in their lower limbs.
- **Poorly-ambulatory individual:** individuals with pathological gait who have some motor function in their lower limbs, but not enough motor function to be considered able-bodied.

Acronyms used to describe impairments:

- **MS:** Multiple Sclerosis
- **CP:** Cerebral Palsy
- **SCI:** Spinal Cord Injury

Acronyms used to describe assistive devices:

- **AFO:** Ankle-foot orthosis
- **KAFO:** Knee-ankle-foot orthosis

Terms that used throughout this thesis to describe a controller's properties:

- **Assistance**: control torques or forces that supplement the user's movement effort. Assistance implies any control action that occurs in the tangential direction to a leg's desired travel path.
- **Guidance**: control torques or forces that guide the user's leg through a desired path. Guidance implies any control action that occurs in the normal direction, and towards the leg's desired travel path.
- **Forgiveness**: a controller's capacity to allow large deviations (error responses) from a desired path. Typically defined as torques (or impedance) properties of a controller when deviating from desired behavior. Forgiveness occurs when error readings are large, whereas guidance refers to torques that guide the user's leg when the leg is close to the desired path (i.e., error is low).

# CHAPTER I

# INTRODUCTION

Ambulatory disabilities are impairments in which a person has serious difficulty moving from one location to another without the aid of assistive devices or mobility aids. Poorly-ambulatory individuals are characterized by inconsistent and underpowered leg movements that arise from weaknesses in the musculoskeletal system. The ability to walk unassisted has a direct correlation with an individual's health, independence, community dwelling capability, and quality of life. The combination of impaired balance and compromised walking decreases an individual's ambulatory capabilities, and increases the incidence injuries resulting from walking. Other factors such as mental health can be correlated to the ability to walk independently (Forster and Young 1995; Harris et al. 2005; Mackintosh et al. 2005; Michael, Allen, and MacKo 2005; Weerdesteyn et al. 2008; Pouwels et al. 2009; Batchelor et al. 2010). Given that being independently ambulatory has a large impact on a person's life, investigating how to improve therapeutic and assistive methods for people to walk on their own is important for the mental and physical well-being of individuals with ambulatory disabilities.

## 1. Gait rehabilitation and passive assistive devices

Rehabilitation for individuals with lower-limb disabilities is administered to re-establish leg movement coordination during walking. Such physical therapy generally includes overground gait training, in which a physical therapist provides balance support (typically via a gait belt) for a patient while assisting the patient with walking (Belda-Lois et al. 2011). In cases where the patient's leg movement is substantially impaired, a physical therapist will manually guide the patient's paretic leg through the gait cycle to encourage a desired pattern of movement, an example of which is seen in Figure 1.

Passive wearable assistive devices for people with ambulatory disabilities include AFOs and KAFOs. These are used to improve joint stability for individuals who have problems supporting their own weight while walking. The subject in Figure 1 is wearing an elastic wrap around the ankle to simulate an AFO to provide stability and prevent foot drop. Some

KAFOs also include stance locking to prevent knee buckling. Most assistive devices in the market are passive devices which do not provide any active power to the user's leg. Thus, a gap exists with wearable assistive devices. Powered devices could serve certain populations with ambulatory disabilities better than currently existing passive devices.

Figure 1. Representative photo of conventional post-stroke gait physical therapy.

This document describes control methods for powered exoskeletons acting as both assistive and therapeutic devices. Therapeutic devices are designed to improve a user's gait by improving leg coordination or strength (or a combination of), but may not improve the user's mobility while wearing the device. Therapeutic devices focus on indirect effects, such that the user's walking improves after wearing and using the device. Assistive devices are designed to improve the user's mobility; they focus on direct effects while wearing the device. Although assistive devices may have therapeutic benefits, indirect effects are a side effect rather than the main objective of wearing the device.

## 2. Powered assistive and therapeutic devices

Powered assistive devices have begun to emerge as an alternative to physical therapy; they also have potentially useful applications for individuals with ambulatory disabilities who require powered assistance to one or more leg joints. Robotic-assisted gait therapy (RAGT) systems can be used to assist therapists with the gait retraining process (Mehrholz et al. 2013). Typically, RAGT systems involve a powered robotic manipulator that assists or corrects the user's movement as they walk. Although variations of RAGT exist, most RAGT

systems incorporate a treadmill in combination with robotic manipulation of the patient's legs and some degree of partial body-weight support as a substitute for the manual leg guidance and balance support that would otherwise be provided by physical therapists. Relative to manual assistance, RAGT systems can decrease the number of therapists required to provide gait training, providing a solution for hospitals to more effectively use therapists' time.

When looking at assistive (rather than therapeutic) benefits, powered wearable assistive devices share benefits with RAGT devices. Robots are capable of repeatable and consistent motions; they theoretically are a good fit for people with ambulatory disabilities, a population largely characterized by inconsistent or weak leg motions. Robots can offer a higher dosage of therapy to patients in a rehabilitation setting when compared to a therapist, or supplement a user's movement to lower fatigue, improve gait kinematics, and increase ambulatory capabilities. The effectiveness of these devices hinges on adequate mechanical design and control. This research has focused on how to more effectively control powered orthotic devices for therapeutic and assistive applications.

## 3. Control strategies for powered exoskeletons

For purposes of this document, lower-limb exoskeletons are defined as powered wearable robotic devices that provide lower limb movement assistance during locomotion. This includes exoskeletons incorporated into treadmill-based systems, body-weight-supported devices (i.e., devices that use harnesses to support the user's weight), as well as overground exoskeletons.

Traditional lower-limb exoskeleton control can be loosely grouped into four categories: electromyography (EMG), trajectory, torque-pulse, and path control. The ideal use of each control strategy is dependent on the user's level of ambulation. Note that stance phase torques are not a defining characteristic of torque-pulse and path control, but rather use a different control rubric for applications such as knee support. Hip torques are rarely employed during stance phase, as the leg impedance is much larger than the user's upper limb and can cause the user's trunk to rotate backwards (i.e. posteriorly), rather than extend the hip.

### 3.1. EMG control

EMG-based control uses EMG readings from the user's thigh and shank muscles to determine the timing and torque applied by the exoskeleton. EMG control approaches are not ideal for non-ambulatory or poorly-ambulatory individuals since they rely on robust, healthy signals from the user's neuromuscular patterns that are not present in people with ambulatory disabilities. However, This type of exoskeleton control has been shown to be robust for use on healthy individuals and has potential to be used in human augmentation techniques for a variety of activities (Sawicki and Ferris 2009; Kawamoto et al. 2003; He and Kiguchi 2007; Fleischer et al. 2006; Yin, Fan, and Xu 2012; Aaron J. Young, Gannon, and Ferris 2017). Further, EMG control methods require substantial interfacing with the user's leg and additional instrumentation than those used in other control strategies. Additionally, EMG control set up can be inadequate for some poorly-ambulatory populations since they suffer from reduced cognitive abilities as a result of their disabilities. Individuals are less likely to adopt EMG control because of the donning process. As a result, EMG control approaches are not considered suitable for purposes of this work.

### 3.2. Trajectory control

Trajectory-based control is a time-based position control that moves the user's leg through a pre-determined path; it is typically employed to for applications where stiff guidance and assistance are required (i.e., non-ambulatory individuals). Trajectory control is the most rigid of the four controllers defined in this document, which makes it the least forgiving. Trajectory control is frequently employed on non-ambulatory users since non-ambulatory populations have no leg mobility, and any volitional leg movement would interfere with the exoskeleton's motions. Trajectory control is a rigid control strategy which will correct any deviations from the path, and will overpower poorly-ambulatory and healthy users if they attempt to deviate from the path. Further, it is a time-dependent controller which makes the user incapable of selecting step time. As such, the user must cede lower limb movement entirely to the exoskeleton.

Some exoskeletons that employ trajectory control are: the ReWalk, created by ReWalk Bionics, based off Israel (Esquenazi et al. 2012); Ekso by Ekso Bionics, based off California,

United States (Bionics 2016); Indego exoskeleton, created at Vanderbilt University and licensed to Parker-Hannifin, based off Ohio, United States (Farris et al. 2012); MINA exoskeleton, developed by the NASA Johnson Space Center and the Florida Institute for Human & Machine Cognition (IMHC) in the United States (Neuhaus et al. 2011); and MINDWALKER exoskeleton, developed in the University of Twente in the Netherlands (S. Wang et al. 2015). Typically, these overground exoskeletons that use trajectory control for non-ambulatory users allow the users to balance themselves using two forearm crutches while the exoskeleton moves the user's limbs during walking. The H2 exoskeleton uses trajectory control with six actuated joints (bilateral hip, knee, and ankle) instead of passive ankle joints (Bortole et al. 2015). Note that the H2 exoskeleton was used for people with stroke (poorly ambulatory), despite being a trajectory controller.

Another type of trajectory control is Zero-Moment-Point control (Kajita et al. 2014). This type of control is employed by the REX exoskeleton. Bipedal walking consists of alternating periods of stability (double support) and instability (single support). The REX exoskeleton uses this control strategy, which deviates from most other commercially available exoskeletons (Barbareschi et al. 2015).

### 3.3. Path control

Control strategies for hip and knee powered exoskeletons can employ path control, otherwise known as "force field control". Path control employs a passive virtual spring-damper system that guides the user's leg motion during gait. This leg guidance can occur at the ankle joint in Cartesian space through an end-effector manipulator, or in configuration-space by controlling the hip and knee joint angles. The leg's desired path is pre-defined by the controller, and the spring component of the path controller corrects for the difference between the user's current leg position and the desired path through a proportional gain. A damper is used for stability purposes and to reduce oscillatory behavior in the leg.

Path control is an inherently passive, time-independent controller. The controller stores potential energy in the spring component, and dissipates energy through the damper. Thus, a path controller does not add energy to the user-exoskeleton system. This feature allows the exoskeleton to guide the user's leg without creating oscillations, if overdamped or critically damped. Since the controller is time-independent, the user can select the walking speed.

Path controllers had been used in treadmill training exclusively until this work's adaptation of the overground path controller (Chapter III). The Active Leg Exoskeleton (ALEX) uses end-effector actuation to guide the user's ankle using a virtual tunnel with a dead band (Banala et al. 2009). The ALEX has the ability to assist the user by providing a torque proportional to how close the user's ankle is to the desired path (lower error to desired path creates larger assistive torques). The Lokomat uses configuration space to guide the user's hip and knee with a dead band (Duschau-Wicke et al. 2010). Lokomat uses a static torque along the desired path to assist the user along the gait cycle regardless of error. Note that despite providing assistance, the controllers are time-independent, as the assistive torques do not constrain the user's gait cycle completion time (though they decrease the swing phase completion time).

### 3.4. Torque-pulse control

Control strategies that focus on correctly timing assistance to the user during walking based on pattern recognition are called torque-pulse control (also known as phase-based oscillator control). Torque-pulse control, unlike trajectory control and path control, provides no guidance to the user's leg; it provides assistance at specific times during the gait cycle. These assistance torques usually occur during early swing and late swing, depending on the powered exoskeleton joints. Torque-pulse controllers seek to improve the user's toe ground clearance and facilitate heel strike for the user.

Torque-pulse control is common in powered single-joint exoskeletons, and is sometimes used in powered exoskeletons with more than one joint. Since it does not provide guidance torques to the user, torque-pulse control is a safe control strategy to use on overground devices.

A formulation for torque-pulse control is detailed by Sugar et al. and implemented in a powered ankle (Sugar et al. 2015; De la Fuente, Sugar, and Redkar 2017). This type of control has been further implemented on a powered hip-only, knee-only, and ankle-only orthosis (Ward et al. 2012; Lerner, Damiano, and Bulea 2017). Similarly, it has been used in powered multi-joint exoskeletons (De la Fuente, Sugar, and Redkar 2017; Murray et al. 2015). The application of torque-pulse control can also be seen in soft exosuits that provide steady-state walking assistance (Quinlivan et al. 2017; Bae et al. 2015). Torque-pulse control

has been also used along with movement primitives to allow for better timing and magnitude of applied torques to the user (Garate et al. 2017).

## 4. User-Balance-Control

With regard to balance, wearable exoskeletons typically use either of two types of strategies: 1) ones for which the primary means of balance control is effected through the user's upper body; and 2) ones for which the primary means of balance control is effected through the user's lower body.

The first type, herein called upper-limb User-Balance-Control (UBC), is applicable to individuals with severe lower-limb neuromuscular impairment but with minor or no upper-limb neuromuscular impairment (e.g., individuals with motor-complete paraplegia). Such individuals are likely non-ambulatory without the use of an exoskeleton or other assistive device, and require the use of a bilateral stability aid such as a rolling walker or a pair of forearm crutches to maintain balance when using an exoskeleton, as seen in Figure 2.

Figure 2. Photo of an individual using the a lower-limb exoskeleton that employs upper-limb user-balance-control.

The second type of balance control, herein called lower-limb UBC, is relevant to individuals with non-severe lower-limb neuromuscular impairment, such as persons with MS, CP, iSCI, or hemiparesis from stroke. Such individuals may use a stability aid such as a quad cane to walk, but are generally able to walk without the use of an exoskeleton or other assistive device, as seen in Figure 3. The objective of the exoskeleton when assisting poorly-ambulatory individuals is to improve the quality of their legged locomotion.

Figure 3. Photo of an individual using the Indego exoskeleton while employing lower-limb user-balance-control.

The distinction between upper-limb UBC and lower-limb UBC for overground walking is important with respect to how a lower-limb exoskeleton provides movement assistance. In the case of upper-limb UBC, the exoskeleton need not cooperate with user-generated lower-limb efforts, and therefore has complete control authority with regard to leg movement.

# CHAPTER II

# CONTRIBUTIONS

The broad goal of this research is to design controllers for powered lower-limb exoskeletons to be used by poorly-ambulatory individuals during overground walking. The specific design goals for the controllers are to allow step time and step length variability so that the subject is able to maintain balance through micro-adjustments in their gait, in addition to the user being active (i.e., the exoskeleton reacts to the user's gait rather than the exoskeleton moving the user's legs by itself).

## 1. Transition path controller to overground walking

The specific aims for the first part of this research are to design a controller that:

- Enables overground walking by allowing the user to select step length and time;
- Guides the user's leg to promote healthy-like gait kinematics;
- Allows the user to be active during walking.

Overground walking is a mandatory feature of assistive devices and is a favorable property of rehabilitation devices as it mirrors what users do in their daily lives. Further, some poorly-ambulatory users have lower cognitive abilities than healthy age-matched populations. A controller that allows users to walk without much cognitive engagement is fundamental for the subjects to adopt and use the controller.

Given these specific aims, the first contribution of this work is to transition a path controller to overground walking for use in the Indego exoskeleton. Typically, controllers for non-ambulatory population have been treadmill bound for several reasons: 1) some patient populations can benefit from carrying lower body weight, since they would not be able to walk otherwise; 2) lower liability of the device (users can't fall to the ground), which increases trust in the device; 3) potentially reduces torque and degree-of-freedom requirements from the robot. Path controllers naturally constrain the user's step length, and

previous iterations have used a treadmill in their system that constrain the user's walking speeds (Banala et al. 2009; Duschau-Wicke et al. 2010). Transitioning to overground walking requires the user to vary either step time or length (Y. Wang and Srinivasan 2014; Danion et al. 2003). As such, adaptation to path controller requires changes to the controller, as previous iterations constrain the gait cycle during both stance and swing phase.

Chapter III of this thesis details the design of a path controller for overground walking. This is the first time (as of June 2019) that a path controller has been adapted to overground walking. The major benefit of an overground path controller is that it is more representative of what users would do in their daily lives. As such, users are more likely to accept treatment when they can ambulate rather than be constrained to a treadmill.

## 2. Design of the velocity-based 'Flow' controller

The specific aim for the second part of this work was to further improve overground walking controllers for a powered bilateral hip and knee exoskeleton. To do this, a new controller was designed with three desired characteristics:

- Provide assistance-as-needed to the user;
- Guide the user's leg to mimic healthy-like kinematics;
- Be forgiving to the user.

Assistance as-needed is important for poorly-ambulatory individuals to complete the gait cycle, and the controller should supplement their movements. Guidance is required to encourage a healthy movement. Additionally, guidance can assist poorly-ambulatory users with ground clearance issues when walking overground. Similar to the path controller, the controller should correct users' gait kinematics to allow for enough ground clearance when walking. Finally, forgiveness means allowing for large deviations from the desired leg path are sometimes needed to maintain balance. Corrective torques applied to the user when deviating from a desired path may create a trip hazard. Potential energy storage in the spring component of path controllers is not a major issue for treadmill-bound controllers, as they support the user's body weight and the user is unable to fall. Unlike treadmill-bound

controllers, an overground walking controller should allow users to relearn balance by allowing them to change their step length when they choose to.

The contribution of the second part of this work is to fill the gap between the path and torque-pulse controllers, such that a single control strategy can provide desirable guidance, assistance, and forgiveness properties to the user. The path controller developed in Chapter III provides guidance. However, the controller lacks assistance capabilities, and due to the virtual spring (and its potential energy storage) is unforgiving to deviations to the desired path. On the other hand, torque-pulse controllers provide assistance-as-needed at specific times during the gait cycle and are forgiving (due to providing no guidance torques).

A secondary aim of this work is to create the control strategy as a uniform control methodology (unlike path controllers, which intrinsically provide guidance, but have an extrinsic control strategy that provides assistive torques). This reduces the amount of variables that therapists or orthotists have to calibrate on the controller.

## 3. Single degree of freedom flow controller

The specific aims for the last part of this work were to:

- Examine if the flow controller is effective in a single degree of actuation system;
- Adapt the flow controller to a KAFO with a powered knee;
- Better understand which individuals with hemiparesis following stroke are suited for the controller

The last contribution of this work focuses on adapting a controller to a single degree of freedom for the knee joint to use on subjects who have hemiparesis following stroke. This contribution can serve as a platform for future controllers to follow based on the control architecture and the use of sensor fusion to calculate the thigh angle over swing phase. The first two contributions of this dissertation focused on a control for a powered hip and knee exoskeleton. Said exoskeleton is a suitable development platform for controllers as having more joints is favorable for control of an individual's walking. However, in applications outside the lab, poorly-ambulatory individuals are more likely to adopt a device that is light

and easy to don and doff.

Another goal of this contribution is to be able to adjust the flow controller for different subjects' pathological gait by modulating two fundamental gains in the controller and adjusting the state transitions to the user's gait. Further, a minor goal of this contribution is to understand which subjects are best suited to use the controller with a Modified Ashworth Scale evaluation prior to walking with the controller.

Note that the third contribution exclusively evaluates the controller as an assistive technology (i.e., improves the user's gait while wearing the device), whereas the first two contributions deal with a controller that can be used for rehabilitative purposes with the goal to improve the user's gait after wearing the device.

# CHAPTER III

# ADAPTATION OF A PATH CONTROLLER TO OVERGROUND WALKING

Approximately 795,000 people in the United States suffer a stroke annually, of which about 665,000 survive (Go et al. 2014). Of these survivors, approximately 200,000 are affected by lower-extremity hemiparesis to an extent that prevents walking without assistance six months after the stroke (i.e., by the time they enter the chronic stages of stroke) (Bogousslavsky, Van Melle, and Regli 1988; Jorgensen et al. 1995; Kelly-Haynes et al. 2003). As mentioned previously, the inability to walk unassisted has an obvious impact on an individual's health, independence, community dwelling capability, and quality of life (Forster and Young 1995; Harris et al. 2005; Mackintosh et al. 2005; Michael, Allen, and MacKo 2005; Weerdesteyn et al. 2008; Pouwels et al. 2009; Batchelor et al. 2010).

In order to address and improve these gait deficiencies, patients are treated with physical therapy intended to re-establish leg movement coordination during walking. Such physical therapy includes overground gait training, in which a physical therapist provides balance support (typically via a gait belt) for a patient while assisting the patient with walking (Belda-Lois et al. 2011). In cases where the patient's leg movement is substantially impaired, this activity is often supplemented by an additional physical therapist, who manually guides the patient's paretic leg through the gait cycle to encourage a desired pattern of movement.

Several robotically-assisted gait training (RAGT) systems have recently been developed, which can assist therapists with the task of gait retraining (Mehrholz et al. 2013). Although variations exist, these systems commonly incorporate a treadmill in combination with robotic manipulation of the patient's legs and some degree of partial body-weight support as a substitute for the manual leg guidance and balance support that would otherwise be provided by physical therapists. Relative to manual assistance, RAGT systems can: 1) decrease the number of therapists required to provide gait training; 2) potentially offer a higher dosage of therapy to the patient; and 3) offer greater consistency of movement, relative to manual gait retraining.

Several control approaches have been described for purposes of governing the interaction

between the robotic manipulation and the patient when providing gait retraining following stroke with RAGT devices, as outlined in (Marchal-Crespo and Reinkensmeyer 2009). Among these are compliant assistance approaches based on spatiotemporal reference trajectories, implemented in the joint space (Aoyagi et al. 2007) or task space (Vallery et al. 2008), which compliantly encourage a step path and step time; path-based approaches (Duschau-Wicke et al. 2010; Vallery, Duschau-Wicke, and Riener 2009; Banala et al. 2009), which compliantly encourage a step path without imposing control forces associated with step time; and torque-pulse approaches that adapt to step frequency, and thus provide assistance without enforcing either step path or time (Ronsse et al. 2011; Lenzi, Carrozza, and Agrawal 2013).

Recently, lower-limb exoskeletons have begun to emerge. Among the differences relative to most treadmill-based RAGT systems, lower limb exoskeletons offer the potential for overground (rather than treadmill-based) gait training. As such, overground exoskeletons can potentially expand the continuum of interventions available to therapists and patients for the treatment of walking impairments. Among the important differences, overground gait training presumably offers a better representation of home and community ambulation (relative to treadmill walking), and may provide benefits with respect to relearning balance during locomotion. Recall that conventional overground gait training typically employs one physical therapist to assist with balance, and often a second to assist with leg guidance. If a lower limb exoskeleton can instead provide the function of leg guidance, then a single physical therapist can perform the simultaneous balance and leg guidance functions that would otherwise require two. Specifically, balance assistance would still be provided by the single physical therapist using a gait belt, but the lower limb exoskeleton, rather than an additional therapist, would provide guidance of leg movement (i.e., facilitate coordination of movement between joints).

As with treadmill-based RAGT devices, control methods are required to govern the interaction between the exoskeleton and patient during overground walking. A number of control strategies have been described for the general control of lower limb exoskeletons (e.g., see the recent review (Yan et al. 2015)). As summarized in that review, lower limb exoskeleton control strategies described for purposes of providing legged mobility to individuals with substantial gait impairments have uniformly been of the trajectory control

type (e.g., (Quintero, Farris, and Goldfarb 2012; Bortole et al. 2015; S. Wang et al. 2014)). Trajectory control is effective at enforcing a given leg movement, but interferes with a user's ability to select step time and length, and thus requires that the patient use a stability aid to maintain balance during walking. In the case of gait retraining after stroke, re-learning of balance is important (Michael, Allen, and MacKo 2005). Re-learning of balance presumably requires a patient to experience states of imbalance, and to select a step length and time to correct for it. Murray et al. (Murray et al. 2015) describe a lower limb exoskeleton controller intended to facilitate overground gait training for individuals with hemiparesis from stroke where the controller does not impose a step time or length. That controller facilitates overground walking by assisting individuals at specific times during the gait cycle (in a similar manner to torque-pulse controllers). However, the controller does not provide desired patterns of movement (i.e., leg guidance) as would a physical therapist when manually guiding leg movement.

In order to address the gap of imposing a desired movement coordination for lower-limb exoskeletons during overground walking, this chapter proposes a controller that is intended to govern the interaction between the exoskeleton and patient during overground walking in a manner that offers a desired inter-joint coordination (i.e., leg guidance), while still enabling a patient to select step time and length. The proposed controller could be used with a stability aid, as per patient needs, but would not require one. The proposed controller specifically employs a path-based approach (to enforce a desired inter-joint coordination without enforcing step time), supplemented with a step-to-step path adaptation that enables step-to-step variation in step length. In order to provide an assessment of the ability of the controller to encourage a desired movement without substantially interfering with balance, the control approach was implemented on a lower limb exoskeleton and assessed in an experimental protocol involving five healthy subjects, who walked overground at varying speeds, without using a stability aid.

## 1. Controller design

The controller is intended to provide leg guidance during walking, as would a physical therapist. The authors conjecture, however, that while leg guidance may be appropriate and helpful during the swing phase of gait, a controller that provides a support function

(particularly at the knee) may be more appropriate for the stance phase of gait. As such, the guidance controller described here is only active during the swing phase of gait, in much the same way a physical therapist typically provides leg guidance during swing (and sometimes knee "blocking" during stance). Note that the controller described here could easily be supplemented by a stance support function, such as a passive "soft stop" around the knee during stance. Such a function, however, is tangential to the focus of this chapter, which is to propose and assess a controller that can provide leg guidance during swing (i.e., "reshape" gait) while still enabling a user sufficient degrees of freedom in the control of his or her lower limbs to maintain bipedal balance.

### 1.1. Torque field

In order to provide leg guidance during the swing phase of walking, while also enabling the user to control step-to-step variation in step time, the controller incorporates a time-invariant force-field-based path-control approach, similar to the approaches previously described for RAGT treadmill-based systems by (Duschau-Wicke et al. 2010; Vallery, Duschau-Wicke, and Riener 2009; Banala et al. 2009). In such path-based control approaches, the exoskeleton controller implements a torque field that imposes a time-invariant coordination between the ipsilateral knee and hip joints. The torque field is defined as follows. Let $\vec{\theta} = [\theta_h, \theta_k]$ be an element of $R^2$ and let $f(\vec{\theta})$ be a plane curve in $R^2$, where $\vec{\theta}_c$ are all $\vec{\theta}$ that satisfy $f = 0$. A representative curve $f$ is shown in the $R^2$ (joint angle) space in Figure 1, which specifically depicts the nominal coordination between the hip and knee angles during normal level walking (as given by (Winter 1991)), where swing phase is shown as a solid line and stance as a dashed line. For each point $\vec{\theta}$ in $R^2$, the corresponding point on the curve $f$ is the $\vec{\theta}_c$ that corresponds to the smallest Euclidean distance from $\vec{\theta}$ to $f$: $\vec{\theta}_c$ satisfies $|\vec{e}| = min|\vec{\theta}_c - \vec{\theta}|$. The error vector associated with $\vec{\theta}_c$ is given by $\vec{e} = \vec{\theta}_c - \vec{\theta}$, which points in the normal direction towards $f$. The normal unit vector is calculated as $\hat{n} = \frac{\vec{e}}{|\vec{e}|}$. The applied control action is a torque vector, $\vec{\tau} = [\tau_h, \tau_k]$, given by:

$$\vec{\tau} = k\vec{e} + b(\vec{\omega} \cdot \hat{n}) \quad (1)$$

where $\vec{\omega}$ is a vector of the joint velocities, $k$ is the stiffness associated with the torque field

and $b$ is the field's damping coefficient. In order to provide a tunnel width, within which no torques will be applied, a small angular distance can be subtracted from the normal component of motion as follows:

$$\begin{cases} e_{db} = \left|\vec{\theta}_c - \vec{\theta}\right| - \delta & if\ |\vec{e}| > \delta \\ e_{db} = 0 & otherwise \end{cases} \tag{2}$$

$$\vec{\tau} = k e_{db} \hat{n} + b(\vec{\omega} \cdot \hat{n}) \tag{3}$$

where $\delta$ is the half width of the tunnel. Figure 4 shows the curve $f$ with a gray band around it, where the width of the band is $2\delta$.

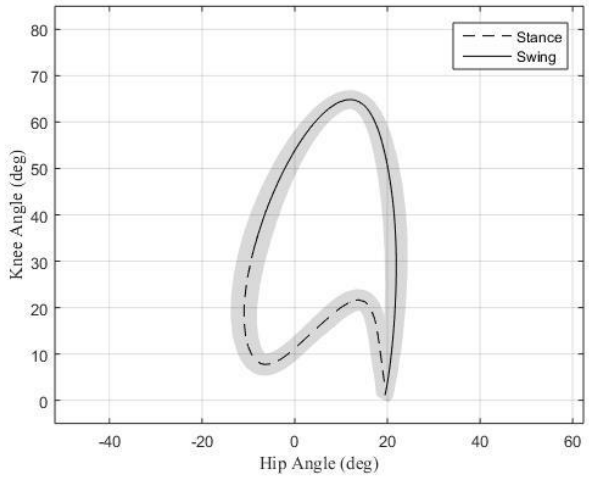


Figure 4. Healthy gait according to Winter's normal cadence walking data.

### 1.2. State machine

In order to distinguish the swing phase from stance phase, the controller employs a two-state state machine, as shown in Figure 5, in which the state transitions between stance and swing are determined by hip and knee joint angles and angular velocities. The state transition conditions depicted in Figure 5 provided robust identification of the respective states for the healthy individuals assessed here, although implementing the proposed controller in a stroke population may require modification of these state transition criteria. Once a state is

identified by the state machine in Figure 5, the exoskeleton imposes the torque field described by equation (3) during the swing phase of each leg, and imposes $\vec{\boldsymbol{\tau}} = 0$ during stance (i.e., exoskeleton motors are off and subjects backdrive the exoskeleton during stance phase).

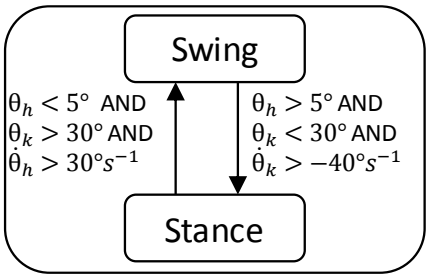


Figure 5. Controller state diagram. Each leg's controller is independent from the other.

1.3. Real-time path variation

Recall the objective of the controller is to provide leg guidance during the swing phase of walking, while still allowing the user to control step-to-step variation in step time and step length. Since the torque field $\vec{\boldsymbol{\tau}}$ is time-invariant and acts normal to the desired path, a user is able to control step-to-step variation in step time. In order to enable step-to-step variation in step length, the path, $f(\vec{\theta})$, is computed in real time at the transition into each swing state. As such, the controller adjusts the path of the "coordination tunnel" based on the leg configuration at the end of stance. Since the user has control of the leg configuration during stance, the user can use this degree of freedom to control step-to-step variation in step length.

In order the generate the path, the controller leverages the fact that the hip/knee coordination exhibited by healthy subjects during the swing phase of level walking, shown in Figure 1, can be closely approximately with the following plane curve:

$$f = K_1{\theta_h}^2 + K_2\theta_h\theta_k + K_3{\theta_k}^2 + K_4\theta_h + K_5\theta_k + K_6 = 0 \quad (4)$$

which is the equation of a standard ellipse, where $K_1$, $K_2$, $K_3$, $K_4$, $K_5$, and $K_6$ are the parameters required to define the ellipse. $K_i$ is defined as:

$$K_i = \det \begin{bmatrix} I_i \\ \Phi_1 \\ \Phi_2 \\ \Phi_3 \\ \Phi_4 \\ \Phi_5 \end{bmatrix} \tag{5}$$

where $I_i$ is the $i$th row of a 6x6 identity matrix ($I_6$), and

$$\Phi_i = \begin{bmatrix} {\theta_{h,i}}^2 & \theta_{h,i}\theta_{k,i} & {\theta_{k,i}}^2 & \theta_{h,i} & \theta_{k,i} & 1 \end{bmatrix} \tag{6}$$

are five vectors defined by the five points ($\vec{\theta}_i = \begin{bmatrix} \theta_{h,i}, \theta_{k,i} \end{bmatrix}$) required to uniquely define an ellipse. For the controller described here, four of the five points ($\vec{\theta}_2$, $\vec{\theta}_3$, $\vec{\theta}_4$, and $\vec{\theta}_5$) are used to enforce the general characteristics of healthy swing phase, as given by (Winter 1991) and shown in Figure 1. $\vec{\theta}_2$ was selected to define peak knee flexion, $\vec{\theta}_3$ is used for shaping the ellipse to match (Winter 1991), $\vec{\theta}_4$ defines maximum hip flexion, and $\vec{\theta}_5$ defines the desired heel strike location. The fifth point ($\vec{\theta}_1$) is computed for each step based on the hip and knee angles at the instant the state machine enters swing (when the three conditions on the left side of Figure 5 are met).

The shape of the elliptical path, relative to the shape of the path defined by healthy walking data (Winter 1991), is shown in Figure 6, which also shows the four points that describe the general shape of the elliptical path, and the nominal torque field, $\vec{\boldsymbol{\tau}}$. Note that for purposes of the figure, damping is assumed to be zero, since the effect of b cannot be otherwise depicted in the $R^2$ space.

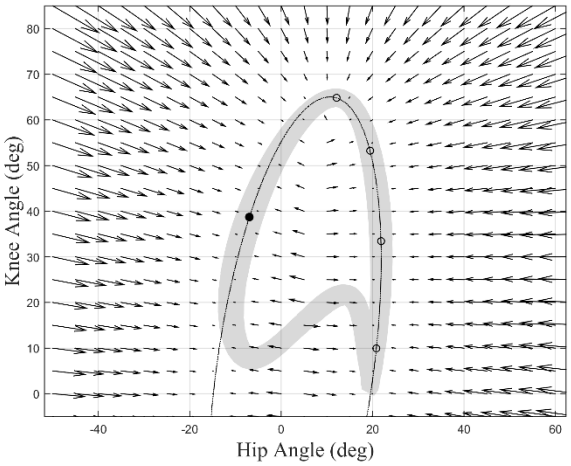


Figure 6. Representation of the ellipse definition and vector field. The unfilled circles along the ellipse are static points chosen from Winter's normal cadence walking data. The location of the filled circle on the left varies depending on the hip and knee angle readings of the toe off state transition. The vector field reflects the controller's action to keep the leg path constrained to Winter's data during the swing phase of gait. The vector field is only active during swing phase.

Figure 7 illustrates the ability of the real-time path calculation to accommodate step-to-step variation in step length. Specifically, the figure shows the plane path $f$, as calculated by equations (4) through (6) and defined by the parameters in Table 1, for the controller implemented on a healthy subject during normal level walking. As can be seen in the figure, the path is reshaped according to the leg configuration when switching into the swing phase, and illustrates a variation in pre-swing configuration greater than the path tunnel width (i.e., greater than the deadband width). In addition to allowing step-length variation, the ability to match the desired path with the entry configuration eliminates step changes in control torques at swing entry, since the initial error between the current and desired paths is zero. The path adaptation feature also more easily accommodates variations between subjects since the path adjusts to the nominal step length of the subject, in addition to adjusting to variations about it.

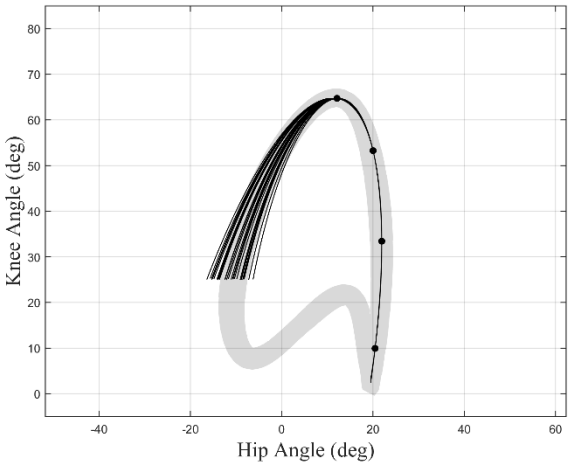


Figure 7. Sections of the ellipses defined from a representative subject's walking data. The adaptable ellipse explicitly accommodates variation in step length.

## 2. Assessment

In order to assess the extent to which the control method provided leg movement guidance during swing, while still allowing bipedal balance, the control approach was implemented in a lower limb exoskeleton, and assessed in an overground experimental protocol involving five healthy subjects. Subjects walked at varying speeds in the exoskeleton without the use of a stability aid, for the case where the guidance controller was active, and also for the case where the controller was turned off (i.e., subjects backdrive the exoskeleton). The following sections describe the implementation and parameterization of the controller, the experimental protocol, and experimental results.

### 2.1. Exoskeleton hardware

The controller was implemented on an open-architecture version of a commercially-available lower-limb exoskeleton (Indego Exoskeleton, Parker Hannifin Corp), shown in Figure 8. Rather than use the commercial control software, the exoskeleton was programmed with software written by the authors to implement the controller described by equations (2) and (3). The exoskeleton hardware platform incorporates four motors for powered movement of bilateral hip and knee joints in the sagittal plane, in addition to built-in AFOs at both ankle

joints to provide ankle stability and transfer the weight of the exoskeleton to the ground. Onboard electronic sensors include encoders at each joint that provide the respective joint angles and angular velocities, and six-axis inertial measurement units (IMUs) in each thigh link, which provide the left and right thigh angles with respect to the vertical. The total mass of the exoskeleton including the battery is 12 kg (26 lbs).

Figure 8. Photo of the Indego exoskeleton.

## 2.2. Controller implementation and parameterization

The controller parameters used in the assessments are given in Table 2, and the parameters used for the parameterization of the nominal ellipse are given in Table 1. Table 2 shows the parameters that authors found with their experience and users' feedback that reshaped gait while minimizing interference with the users' gait. The spring constant value of 9 Nm/º successfully reshaped subjects' gait, while allowing deviations from the desired path. The damping coefficient was selected to be proportional to the square root of the spring constant: $b = 0.08\sqrt{k}$. The deadband was selected to roughly match the standard deviation

between strides during healthy gait. The controller parameters remained the same for all subjects and for all trials. As previously mentioned, the ellipse parameters were selected to fit data from healthy subject walking (i.e., (Winter 1991)), although if used in a clinical setting, the nominal shape would likely be adjusted by physical therapist. Although not explicitly described by equation (3), the damping ratio $b$ was ramped up from zero to the value in Table 1 over the first 75 ms of swing phase to avoid a step change in torque when entering swing. Specifically, although the real-time computation of elliptical path eliminates step changes in position-based torque when entering swing, the function $f$ exists strictly in the $R^2$ joint angle space, and is therefore unable to eliminate step changes in velocity-based torque.

Table 1. Points used for ellipse definition

| Point ($\theta_i$) | Hip Angle ($\theta_{h,i}$) | Knee Angle ($\theta_{k,i}$) |
|---|---|---|
| $\theta_2$ | 12.1° | 64.7° |
| $\theta_3$ | 20.0° | 53.3° |
| $\theta_4$ | 21.9° | 33.5° |
| $\theta_5$ | 20.5° | 10.0° |

Table 2. Controller parameters

| Parameter | Symbol | Magnitude |
|---|---|---|
| Spring Constant | k | 515 Nm/rad (9 Nm/°) |
| Damping Coefficient | b | 13 Nm s/rad (0.225 Nm s/°) |
| Half Tunnel Width | $\delta$ | 0.026 rad (1.5°) |

2.3. Description of experimental comparison cases

The efficacy of the controller, specifically its ability to provide leg guidance while allowing bipedal balance, was assessed in a set of comparative experiments on healthy subjects, who walked overground in the exoskeleton with two different control conditions: a "baseline" condition in which the exoskeleton imposed no control torques, and a test condition in which the exoskeleton was controlled by the previously described controller. In order to succinctly reference these cases, the baseline (i.e., no control torques) is referred to

as the “unguided” case, while the latter (i.e., the test condition) is referred to as the “guided” case. The unguided case, in particular, imposes no control torques but also does not cancel or counteract passive torques such as transmission friction, rotor inertia, and gravitational loads.

However, the inertia of the motor rotors has the effect of altering the shape of the swing phase trajectory from a typical healthy shape (e.g., Figure 4) to a more rounded shape. In this chapter, the authors leverage this alteration in shape. The passive alteration of shape provides an emulation of impairment by moving the uncorrected shape of movement away from the typical healthy pattern. As a result, the authors selected the desired movement shape to reflect typical healthy movement (i.e., the shape in Figure 4). The important aspect for purposes of this chapter is not the extent to which a specific movement can be achieved, but the extent to which the exoskeleton is able to reshape a given movement to a different desired movement, while still allowing a user to maintain balance. If the exoskeleton were perfectly transparent (i.e., perfectly backdrivable), the baseline movement of the healthy subjects would have been healthy movement (i.e., the shape of Figure 4), and the experimental test case would have had to reshape that movement to a different, arbitrary shape. That would have also been a valid test of the control method investigated here; the authors believe, however, the experiments are more representative of eventual use in the form taken here – starting with an abnormal (yet unconstrained) movement, and having the controller reshape movement toward a healthy norm. Finally, it should be noted that, in addition to using a desired trajectory reflective of a healthy norm, the guided case also maintains the same desired shape for the three walking speeds tested (as subsequently described). This can be viewed as unnatural, since these shapes would presumably change somewhat with walking speed. As previously mentioned, however, the specific desired shape is relatively unimportant in this assessment; rather, the important aspect is the extent to which the guided controller is able to reshape joint movement from some unguided shape to some desired shape.

The objective of the experiments is to assess the extent to which the proposed control approach can encourage or enforce a coordination, while still enabling a user to maintain balance. As implied in the discussion, one application of the proposed work is gait retraining following stroke, in which case the user would presumably have hemiparesis, where the

impairment is primarily unilateral. Despite this, since the assessment is conducted on healthy subjects, a bilateral implementation is both more rigorous and more informative, specifically with respect to assessing the extent to which a user is able to maintain balance in the presence of guidance. Specifically, healthy subjects with a unilateral constraint have considerable ability to impose compensatory actions with the contralateral limb. A subject could in essence maintain a severe limp and still maintain balance. A bilateral constraint is therefore a much clearer assessment of the intended objective of the chapter. Further, other impairments (e.g., incomplete spinal cord injury, multiple sclerosis, cerebral palsy) would employ the controller bilaterally. As such, the controller is implemented bilaterally in these experiments.

### 2.4. Experimental protocol

The comparative experiments involved five healthy subjects who walked overground in the exoskeleton at three different speeds, without stability aids, under the two comparative control conditions previously described. The mean age of the five healthy subjects was 25 years, with a standard deviation of 1 year (4 male, 1 female). Data was recorded from a motion capture system for both cases, and the nature and consistency of coordination between the hip and knee angles were compared.

Prior to recording data, subjects were trained to walk in the exoskeleton in the guided condition until they felt comfortable walking in it at various walking speeds. Subjects were required to train for a minimum of one hour, which consisted of walking on a treadmill at a self-selected speed for both the guided and unguided condition (15 min each) and 30 min overground walking (split between the two tested conditions and three speeds). A maximum training time was not specified. Subjects were considered ready to conduct the protocol based on their own and the authors' discretion. Subjects were instructed to cooperate with the exoskeleton guidance in the same manner they would if the guidance were provided manually by a physical therapist.

The experimental protocol consisted of an acclimation period followed by the data collection trials. For both the acclimation trials and the data collection trials, subjects walked 50 meters without a stability aid on an indoor track. The acclimation period consisted of six mock trials, alternating between unguided and guided conditions where subjects walked at

0.6 m/s, 0.8 m/s and 1.0 m/s respectively. The walking speeds were enforced by having subjects walk alongside one of the authors, who set the pace based on six markers distributed over the 50 m length by timing intervals between the markers. All 50 meter trials were completed within 2 s of the target time (i.e., a maximum error of 4% in average velocity). The data collection trials consisted of two identical sets of six trials, ordered as follows: 1.0 m/s unguided, 1.0 m/s guided, 0.8 m/s unguided, 0.8 m/s guided, 0.6 m/s unguided, and 0.6 m/s guided. Each control case at each speed consisted of approximately 200 steps per subject, such that each control case at each speed across all subjects consisted of approximately 1000 steps, and the total data set (two control cases and three speeds) consisted of approximately 6000 steps.

An IMU based motion capture system (Xsens AWINDA) was used to measure hip and knee angles during walking. Note that the exoskeleton also measured hip and knee angles, although because of the soft-tissue interface between the exoskeleton and user, there is necessarily a difference between exoskeleton motion and that of the user, particularly in the presence of control torques. The IMU-based system was used as follows. A lower limb skeletal model was created for each subject using the Xsens MVN Studio 4.2 software. Seven IMUs were employed to create the model: one on the lower back and three for each leg. Figure 9 shows a subject wearing the lower limb exoskeleton and the locations of the Xsens IMUs for the lower back and left leg. The lower back IMU was placed over the subject's sacrum. The upper leg IMUs were located on the inside of the thigh, about six inches above the knee and aligned with the sagittal plane. The shank IMUs were placed on the flat surface over the tibia bone, about four inches below the knee. The foot IMUs were placed on top of the subjects' feet, under the shoe tongue. The skeletal model was calibrated at the start of each trial by having the subject stand up in a neutral pose with knees extended for approximately 5 s, as recommended by the manufacturer. Since each subject's neutral pose differs, all Xsens data was aligned to its respective exoskeleton calibration data, which was kept consistent among all trials. Motion capture data from the Xsens system were collected at 60 Hz. Following data collection, the data were parsed into individual strides based on the state machine transition from swing to stance, as shown in Figure 5, and each stride was then normalized to a stride percentage. The first three strides and the last stride for each leg were not included to avoid transient effects associated with starting and stopping.


Figure 9. Photo of subject wearing the exoskeleton and IMUs. Numbers represent positions of Xsens IMUs at the pelvis (1); thighs (2), shanks (3), feet (4).

# 3. Results

## 3.1. Representative data

Figure 10 shows representative data for the exoskeleton hip and knee angles as measured by the exoskeleton joint encoders. The top plot shows a representative unguided trial, and the bottom plot shows a representative guided trial. The gray band in each plot depicts the nominal coordination tunnel implemented by the controller. Note that the dashed lines in the bottom plot (guided case) indicate stance phase, during which the guidance is turned off. As can be seen from the representative data, the exoskeleton with the guidance controller is able to guide movement of the leg according to the desired swing phase path. Although variation in step time is not readily apparent from the plots, one can observe the variation in step length present in both the guided and unguided data sets, characterized by approximately 10 deg of variation in hip angle at the transition between the stance and swing phases.

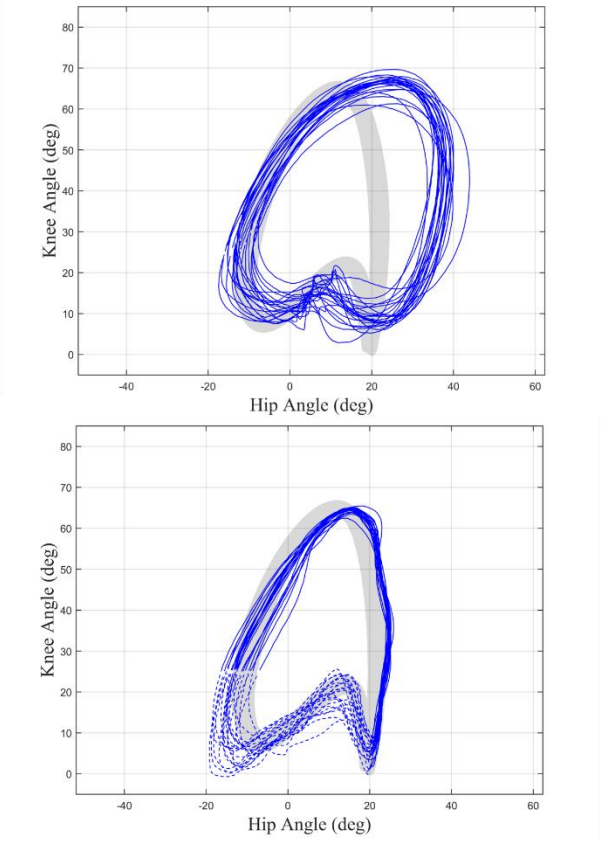


Figure 10. Exoskeleton data for 10 strides during subject 3's left leg during the 0.6 m/s trial. For the bottom graph (guided condition), the dashed line represents stance phase (controller inactive); the solid line represents swing phase (controller active). The controller is inactive for all the data shown in the top graph (unguided condition).

Figure 11 shows similar representative data, also from Subject 3, averaged across all trials and both legs, for each walking speed, for each control case, measured using the Xsens rather than the exoskeleton joint encoders. Note that Figure 10 captures movement of the exoskeleton, while Figure 11 captures movement of the limb (the difference being soft tissue deformation). Specifically, the top row plots show average movement during 50 m of walking, averaged also across both legs, for each of the 0.6 m/s, 0.8 m/s, and 1.0 m/s trials, all without guidance, while the bottom row plots show the analogous data for the trials with exoskeleton guidance, where each gait speed is shown in a different color. The gray band in each plot depicts the nominal coordination tunnel implemented by the controller. Note that the guided cases do not track the nominal path as well as in Figure 10, due to the soft tissue

deformation between the exoskeleton and limb.

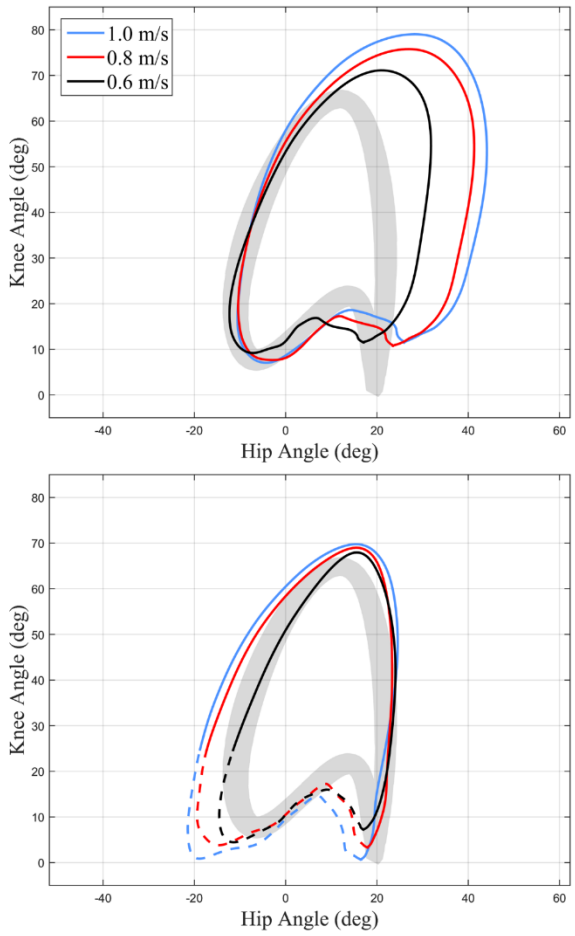


Figure 11. Subject 3's average kinematic data: 0.6 m/s (black); 0.8 m/s (red), 1.0 m/s (blue). For the bottom graph (guided condition), the dashed line represents stance phase (controller inactive); the solid line represents swing phase (controller active). The controller is inactive for all the data shown in the top graph (unguided condition).

### 3.2. RMS guidance error

The extent to which the controller was able to effectively reshape joint movement was characterized by computing the root-mean-square (RMS) difference between the recorded movement and the desired movement. Figure 12 shows the averaged motion capture (i.e., Xsens) data for all subjects and all trials. Specifically, the top row (a, b, and c) shows the averaged left and right leg data for each subject at 0.6 m/s, 0.8 m/s, and 1.0 m/s, respectively,

for the unguided trials, while the bottom row (d, e, and f) shows the analogous data for the guided trials, where each subject is shown in a different color. The gray band represents the nominal coordination, and is shown for reference. Data for the guided cases clearly indicates much greater movement consistency relative to the corresponding unguided cases. Specifically, while each subject employs his or her own movement preferences in the unguided trials (top row), all subjects conform to a similar movement pattern in the guided trials (bottom row).

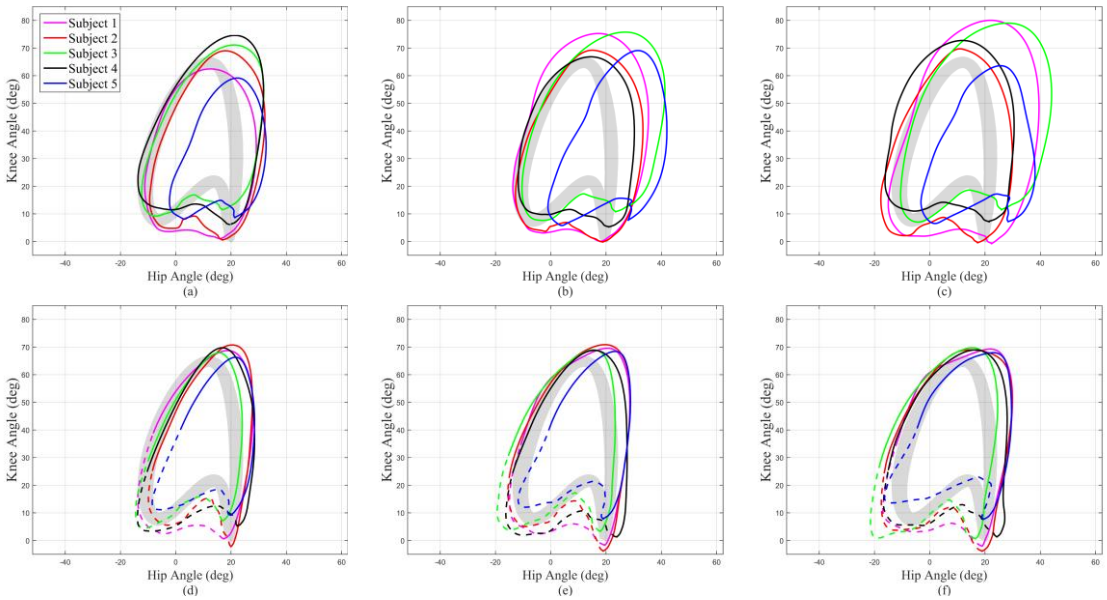


Figure 12. Subjects' averaged kinematic trials data for both legs in the conditions (a) 0.6 m/s unguided; (b) 0.8 m/s unguided; (c) 1.0 m/s unguided; (d) 0.6 m/s guided; (e) 0.8 m/s guided; (f) 1.0 m/s guided. Bottom row (guided condition): the dashed line represents stance phase (controller inactive); the solid line represents swing phase (controller active). The controller is inactive for all the data shown in the top row (unguided condition).

In order to quantitatively characterize the extent of guidance provided by the controller, the RMS error from the joint encoders was computed for each trial shown in Figure 13. Specifically, the RMS difference between the mean path and nominal path (including the deadband) was computed for each subject and each trial. The RMS values for all trials and for all subjects are shown in Figure 16, where the top plot shows the RMS differences for each subject at each speed for the unguided case, and the bottom plot show the RMS

differences for each subject at each speed for the guided case. The mean RMS difference for all subjects during the unguided trials was 7.0, 9.4, and 13.3 deg for the 0.6 m/s, 0.8 m/s, and 1.0 m/s walking speeds, respectively. The mean RMS difference for the guided trials was 0.7, 1.3, and 1.8 deg for the 0.6 m/s, 0.8 m/s, and 1.0 m/s walking speeds, respectively. Unpaired *t*-tests (in which each step was a sample, such that each data set consisted of approximately 1000 samples) were performed comparing the guided and unguided mean RMS differences at each speed. Results show statistically significant differences ($p<0.01$) between the conditions for all walking speeds. Averaged across all subjects and all speeds, the RMS difference in paths was 9.9 deg for the unguided trials, and 1.3 deg for the guided trials. As such, the guided trials demonstrated on average an 8.6 deg reduction in RMS path difference, and 13.1 percent of the error of the unguided trials.

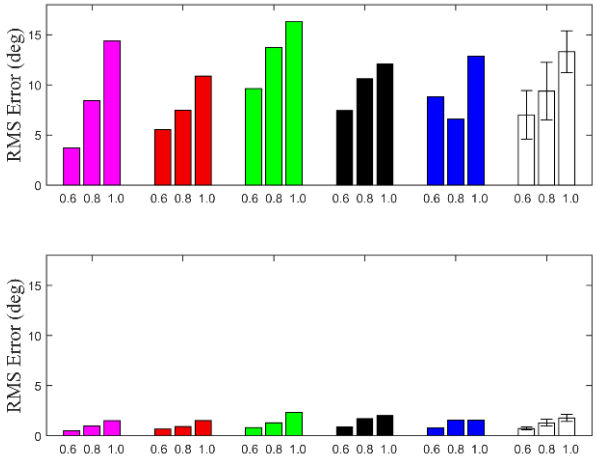


Figure 13. Individual trial RMS errors for exoskeleton's leg path for the unguided and guided trials. First five sets from left to right represent a subject: 1 – pink; 2 – red; 3 – green; 4 – black; 5 – blue. White represents the mean of all subjects along with error bars representing one standard deviation for trials of the corresponding speed.

### 3.3. Variation in step time and length

As previously discussed, the intent of the proposed controller is to provide movement guidance (i.e., to effectively reshape movement, as characterized here by RMS error), while

still enabling a user to maintain bipedal balance via ability to vary step-to-step step time and step length. In order to characterize the ability of the subjects to do so, step time and length for each subject, speed, and control condition were recorded from the IMU motion capture system. These data are collectively summarized in Table 3 (step time) and Figure 14 (step length).

Specifically, Table 3 shows the mean and standard deviation in step time across all subjects for each speed, for both the unguided and guided trials. Note that each entry is the average of approximately 1000 steps, and that paired *t*-tests indicate no differences in means between respective control conditions within a given walking speed. It should also be noted that the step time variability between the unguided (i.e., no constraint) and the guided cases are quite similar. Specifically, the step time variance of the guided control condition was 90%, 93%, and 89% of the step time variance of the unguided case for the walking speeds of 0.6 m/s, 0.8 m/s, and 1.0 m/s respectively. As such, the data indicates that subjects were able to adjust step time when using the controller nearly as freely the case with no control constraints.

Table 3. Mean trial step time between subjects

| Trial (m/s) | Unguided Trial Step Time (sec) | Guided Trial Step Time (sec) |
|---|---|---|
| 0.6 | 0.85 ± 0.11 | 0.88 ± 0.09 |
| *0.8* | 0.74 ± 0.07 | 0.74 ± 0.06 |
| *1.0* | 0.68 ± 0.05 | 0.66 ± 0.04 |

Figure 14 shows the means and standard deviations in step length for all subjects and all trials. The mean step length across all subjects in the guided condition was 0.50 m, 0.59 m, and 0.65 m for the 0.6 m/s, 0.8 m/s, and 1.0 m/s walking speeds, respectively. Note that these values essentially match the step length means of the unguided trials, which were 0.49 m, 0.59 m, and 0.66 m for the 0.6 m/s, 0.8 m/s, and 1.0 m/s walking speeds, respectively. The ensemble average of each subject's intrasubject step length variability, calculated as standard deviation divided by the mean for each subject, was 4.9% and 4.6% for the unguided and guided cases, respectively. As in the step time data, the step length data indicate that subjects were able to adjust step length when using the controller nearly as freely as the case with no

control constraints. It should be further noted that the values measured here and reported in Figure 14, including the intrasubject step length variability, are consistent with step length studies presented in recent literature (Y. Wang and Srinivasan 2014; Danion et al. 2003). The controller required no change to its parameters or settings to achieve the variability of step length seen in Table 3 and Figure 14.

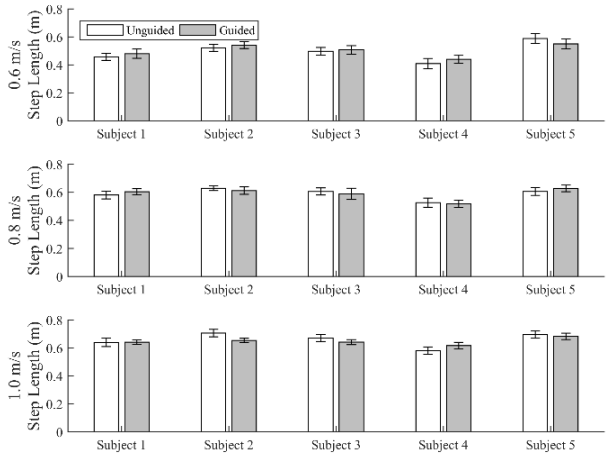


Figure 14. Step length mean and standard deviations for all subjects across all velocities. Data were recorded with Xsens IMUs.

### 3.4. Exoskeleton control torques

Figure 15 shows the hip and knee torques exerted by the exoskeleton as percentage stride for the three walking speeds averaged across all subjects. Note that these torque magnitudes are generally smaller than those observed at the hip and knee during the swing phase of healthy walking (Winter 1991), but of the same order of magnitude. The controller imposes the greatest guidance torques in both joints between approximately 75 and 85% stride, which corresponds to peak hip and knee torques of approximately 40 and 30 Nm, respectively, at the fast gait speed of 1.0 m/s. As such, an exoskeleton must be capable of providing these magntitudes of peak joint torque in order to impose the guidance control constraints used in the experiments described here.

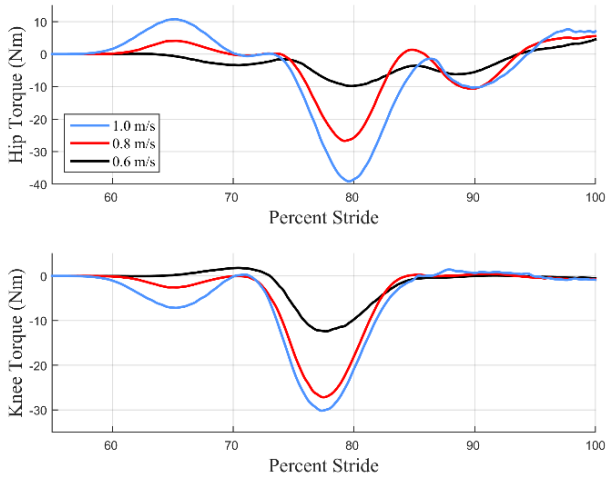


Figure 15. Average exoskeleton torque as percentage stride for the three tested speeds, averaged across all subjects. Note that positive torques are in the flexion, while negative torques are in extension.

### 3.5. State machine performance

Figure 16 provides an indication of the efficacy of the state machine detection of the stance and swing states. The mean timing of all subjects' transition from stance to swing (i.e., toe off state transition) was 61.9 ± 1.5 percentage of stride, which is consistent with previous studies of healthy subject toe off timing (Winter 1991; Perry and Burnfield 2010). The state machine did not miss any transitions in these trials. As previously mentioned, however, in the case that the controller is used on subjects with hemiparesis, it is likely that the state transition conditions will require revision.

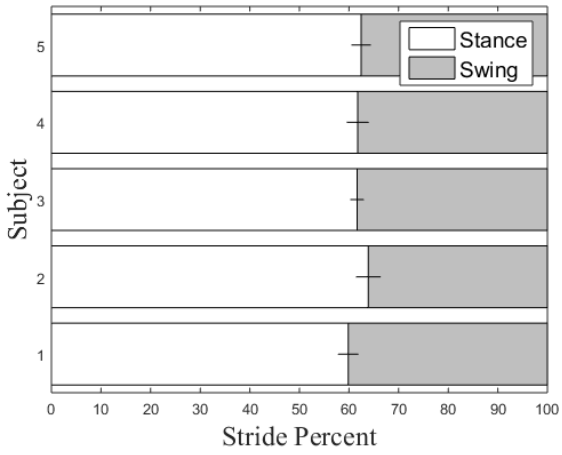


Figure 16. Exoskeleton controller recorded state transitions. The vertical lines represent the swing state transition mean for a subject's guided trials. Horizontal lines denote ±1 standard deviation.

## 4. Discussion

The essential objective of the controller described here is to enforce a desired inter-joint coordination (i.e., a desired leg movement) during swing phase, while allowing for sufficient step-to-step variation in step time and step length to enable control of bipedal balance. Regarding the ability to provide a desired coordination (i.e., a desired path in the joint space), Figures 9 and 10 indicate the efficacy of the controller in reducing the RMS path differences across all subjects and speeds. Regarding the ability to vary step time and length, Table 3 and Figure 14 indicate that subjects were able to vary step time and length, respectively, to nearly the same extent when walking with guidance as when walking without.

Despite the observed similarity in step length variation, the mechanism by which this variation was achieved was not strictly preserved between the unguided and guided cases. Specifically, step length in general is approximately a function of the difference in hip angle between the toe-off and heel strike events. As illustrated in Figure 10, step length variation in the unguided case employs substantial variation in hip angle at both events, while step length variation in the guided case is restricted to occur at toe-off. The extent to which this restriction affects balance is unclear; however, as indicated in the data of Figure 14, this restriction did not substantially affect the magnitude of step-to-step adjustments in step

length between the guided and unguided cases, and did not preclude the ability of all subjects to walk at all speeds without the use of a stability aid.

Regarding the ability of the controller to allow user control of step length, one could potentially assert that, rather than employ the real-time path adaptation proposed here, that step length variation could be accommodated by increasing the width of the tunnel (or deadband) in equation (2), which for the experiments shown here was set to 3 deg (see Table 5). As seen in Figure 7, a typical step-to-step variation in hip angle spans approximately 10 deg (i.e., ±5 deg relative to nominal), and as seen in Figures 7 through 9, the average (nominal) hip angle variation across speeds is also approximately 10 deg. As such, step-to-step hip angle variation across all speeds (tested here) within a single subject requires variation of approximately 20 deg in hip angle. Such variation is an order of magnitude larger than the tunnel width as given in Table 5, and thus clearly not possible using the path width settings employed here. Further, although a path width of 20 deg could be used, using a path width that would accommodate this variation would substantially lessen the efficacy of leg guidance (i.e., coordination between joints would be enforced to a much lesser extent). The use of an adaptive path, as described here, allows for the step-to-step and speed-to-speed variation in step length (i.e., hip angle) required here (by healthy subjects), while enabling a substantially greater degree of swing phase guidance, relative to the alternative of a widened tunnel width.

Finally, although the controller was demonstrated on healthy subjects, the intended objective is to facilitate overground walking recovery in persons with lower limb hemiparesis from stroke. Specifically, as stated earlier, the intent of the controller is to enable a single physical therapist to perform the function of balance assistance, while the exoskeleton provides the function of leg guidance. With a stroke population, several differences in the controller would be expected. First, the controller would most likely be employed in a unilateral manner. Second, one would likely employ support assistance at the knee joint during the stance phase of gait. Third, as previously mentioned, the conditions for state switching between stance and swing would like require revision for the stroke population. Fourth, muscle weakness or spasticity in the stroke population may require the use of assistive torques along with nominal movement path, as opposed to strictly orthogonal to it. Finally, the nominal coordination path would likely be adjusted to be more appropriate

for individuals with hemiparesis. Nonetheless, the results presented here, although on healthy subjects, indicate that the control approach is able to provide leg guidance, while still enabling variation in step time and length similar to that observed without the controller.

## 5. Conclusion

A controller for a lower-limb exoskeleton that provides leg guidance during the swing phase of gait was described and evaluated in this chapter. Kinematic data from five healthy subjects walking in the exoskeleton with and without the guidance controller demonstrates that the controller was able to provide substantial leg guidance, while still enabling the user step-to-step variability in step time and length sufficient to maintain bipedal walking balance without a stability aid. The authors believe the control approach may be useful for purposes of gait retraining following stroke and other neuromuscular impairments, and plan in future work to adapt the controller for such use.

# CHAPTER IV

## FLOW CONTROLLER: A VELOCITY-FIELD-BASED CONTROLLER

Lower-limb exoskeletons are wearable robotic devices that provide lower limb movement assistance during overground locomotion without offering overhead body weight support. These exoskeletons have recently begun to emerge as viable assistive devices for individuals with mobility impairment (Yan et al. 2015; A.J. Young and Ferris 2017; Meng et al. 2015; Chen et al. 2013). Because there has been a recent proliferation of exoskeletons and associated control methodologies, and since the nature of methodologies is dependent on the exoskeleton type, this chapter considers the control of a lower-limb exoskeleton with unilateral or bilateral sagittal-plane hip and knee assistance (i.e., exoskeletons that provide ipsilateral inter-joint coordination). Most control methods for such exoskeletons do not provide balance control, for a number of reasons, including the fact that lower-limb exoskeletons generally lack sufficient sensing and actuation to do so (e.g., exoskeletons typically do not sense the configuration of the human upper-body; lack six degree-of-freedom force sensing under the feet, generally have insufficient actuated degrees of freedom, or control authority, to provide balance control in three dimensions). Further, completely ceding balance control to the machine creates substantial liability concerns, while in the case of balance assistance, conflicting balance control strategies between a user and lower-limb exoskeleton can create a trip hazard. Finally, automated balance control may interfere with or defeat the ability of the user to relearn balance in applications in which that is an objective. As such, in nearly all lower-limb exoskeleton implementations, the onus of balance control is left to the user, rather to the machine.

With regard to such balance control, two types of applications can be considered: 1) ones for which the primary means of balance control is effected through the user's upper body (upper-limb UBC), and 2) ones for which the primary means of balance control is effected through the user's lower body (lower-limb UBC). Upper limb UBC is applicable to individuals with severe lower-limb neuromuscular impairment but with minor or no upper-limb neuromuscular impairment (e.g., individuals with motor-complete paraplegia). Such

individuals are likely non-ambulatory without the use of an exoskeleton or other assistive device, and require the use of a bilateral stability aid such as a rolling walker or a pair of forearm crutches to maintain balance when using an exoskeleton.

Lower-limb UBC is relevant to individuals with non-severe lower-limb neuromuscular impairment, such as persons with MS, CP, incomplete SCI, or hemiparesis from stroke. Such individuals may use a stability aid such as a quad cane to walk, but are generally able to walk without the use of an exoskeleton or other assistive device. For purposes of this work, such individuals are regarded as poorly-ambulatory, and the objective of the exoskeleton is to improve the quality of their legged locomotion.

The distinction between upper-limb UBC and lower-limb UBC for overground walking is important with respect to how a lower-limb exoskeleton provides movement assistance. In the case of upper-limb UBC, the exoskeleton need not cooperate with user-generated lower-limb efforts, and therefore has complete control authority with regard to leg movement. Accordingly, many hip and knee exoskeleton control methods described for use with upper-limb UBC applications are of a predetermined trajectory-control type, such as those described by (Suzuki et al. 2007; Neuhaus et al. 2011; Quintero, Farris, and Goldfarb 2012; S. Wang et al. 2015; Bortole et al. 2015). These methods have been shown to provide effective control for such applications, and are in fact employed in multiple commercially-available lower limb exoskeletons (Esquenazi et al. 2012; Hartigan et al. 2015; Kozlowski, Bryce, and Dijkers 2015).

Although upper-limb UBC approaches are effective for walking assistance in non-ambulatory individuals, they are generally not appropriate for applications involving poorly ambulatory individuals who employ lower-limb UBC. In the case of lower-limb UBC, the individuals use their lower-limb neuromuscular system to provide movement and control of balance. In these applications, the exoskeleton should provide movement assistance to the user (to facilitate improved locomotion), and either cede lower-limb balance control authority to the user, or provide balance assistance. Due to the complexities associated with the latter, this work focuses on providing movement assistance, without introducing balance interference. As such, the objectives of the exoskeleton controller in this work are to: 1) supplement movement effort (i.e., provide movement assistance); 2) encourage a desired inter-joint coordination (i.e., provide kinematic guidance); and 3) allow a user to deviate as

needed from the nominal inter-joint coordination as required to maintain balance (i.e., be forgiving to sudden deviation from a nominal motion). Various control methods have been proposed that provide some aspects of these control objectives. These controllers can be loosely associated with one of two approaches: 1) torque-pulse approaches (e.g., (Garate et al. 2017; Murray et al. 2015; Ronsse et al. 2011; Bae et al. 2015; Lerner, Damiano, and Bulea 2017; Ward et al. 2012; Quinlivan et al. 2017; De la Fuente, Sugar, and Redkar 2017; Sugar et al. 2015)); and 2) potential-energy-based path approaches (e.g., (Banala et al. 2009; Duschau-Wicke et al. 2010; A. Martinez, Lawson, and Goldfarb 2018)). Both have been shown to be effective for overground exoskeleton-assisted walking. Torque-pulse approaches provide effective assistance and inherently allow variation in step time and/or length, but do not explicitly provide kinematic guidance, and therefore do not provide inter-joint coordination in this regard. As such, they provide two of the three aforementioned objectives. Path-based approaches are effective at providing inter-joint coordination (i.e., guidance), and also allow step-time variation (i.e., are forgiving in terms of step time). Path-based approaches, however, do not implicitly provide assistance (although assistive components can be separately included), and more importantly, as discussed later in this chapter, are not generally forgiving to step-length variation. As a result, they can create a trip hazard.

An additional approach that has been used effectively is electromyogram (EMG) based control methods (Sawicki and Ferris 2009; Kawamoto et al. 2003; He and Kiguchi 2007; Fleischer et al. 2006; Yin, Fan, and Xu 2012; Aaron J. Young, Gannon, and Ferris 2017). Such methods are not considered here since they require additional (EMG) interface and instrumentation. EMG control approaches are not always well-suited to individuals with neuromuscular impairment. Rather, the control methods considered here rely strictly on sensors within the exoskeleton that need not make contact with the user's skin or rely on healthy neuromuscular patterns.

In order to better provide the three aforementioned objectives of movement guidance, assistance, and forgiveness to poorly-ambulatory individuals, the authors propose here an exoskeleton controller that offers these characteristics by simulating a fluid flow field that influences limb movement via virtual viscous interaction between the virtual flow field and the user's legs. The controller is called a flow controller. Because the flow controller does

not store potential energy as a function of path error, it is inherently more forgiving than a path-based approach. The absence of such potential energy storage reduces the effect of previous path errors on the control effort, and thus results in a controller with a smaller disturbance transfer function. In this chapter, the flow controller formulation is described, and the ability of the controller to provide the previously-stated control objectives is tested by implementing the flow controller in a lower-limb exoskeleton and comparing its characteristics to a previously-published path controller in experiments on five healthy subjects.

## 1. Controller design

The authors previously described a path controller where the fundamental guidance component was derived from the gradient of a potential-energy-field (A. Martinez, Lawson, and Goldfarb 2018), similar to other previously-published path-type controllers (Banala et al. 2009; Duschau-Wicke et al. 2010). Note that this controller type is probably more accurately referred to as a potential field controller, but "path" controller is used here for brevity. The flow controller presented in this chapter was derived to provide path-like guidance, but without the stored potential energy and corresponding restoring forces that result from path deviation. In order to provide context for the behavior of the flow controller, comparative experiments were conducted with the same set of subjects using both the path and flow controllers. As such, the control behavior of both controllers is presented here. Note that both controllers employ the same general control structure, where the main difference is the constitutive behavior of the respective torque fields applied by each. Specifically, both are governed by the same two-state controller for each leg, and both employ the same stance-phase behaviors. Both also employ field-type swing-phase behaviors, and both incorporate the same joint-space desired path. As such, the only difference between the two controllers is the specific description of the torque vector as a function of configuration space, as given in the previous chapter for the path controller, and in (6) and (7) for the flow controller.

### 1.1. State machine

Both the path and flow controllers provide guidance in the swing phase of walking,

where the swing versus stance behaviors are selected by the state machine depicted in Figure 17. The conditions for switching between stance and swing states are based on hip and knee angles, where a positive value indicates flexion, and angular velocity signals determine the state transitions. Note that, for both switching conditions, the state switches based on the angular velocity condition (i.e., hip begins flexing or knee stops extending, respectively). The angle conditions are effectively guard conditions that limit the regions of the configuration space in which switching can occur. Both legs use the same state transitions and operate independently from one another.

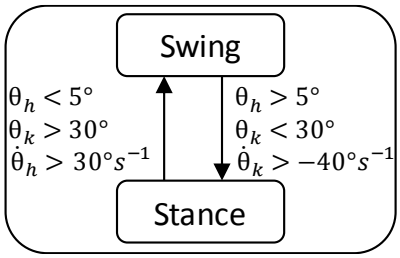


Figure 17. Controller state machine diagram. Each leg's controller is independent from the other.

1.2. Swing phase control

The swing phase control for both control laws is described in the configuration joint space, which for each leg is given by the vector:

$$\vec{\theta} = (\theta_{hip}, \theta_{knee}) \tag{7}$$

where $\theta_h$ and $\theta_k$ are the hip and knee joint angles, respectively, and the vector $\vec{\theta}$ is referred to as the configuration. Hip joint angle ($\theta_h$) is positive in hip extension and negative in flexion. Knee joint angle ($\theta_k$) is positive in knee extension and negative in flexion. The time derivative of the configuration is given by:

$$\vec{\omega} = \frac{d\vec{\theta}}{dt} \tag{8}$$

In both controllers, a desired set of configurations defines a desired path in the

configuration space (e.g., a path representative of healthy or otherwise desired movement). A nominal desired path, in this case representing movement during healthy walking (Winter 1991), is shown in Figure 18, which the solid line is the swing phase movement and dashed is stance phase.

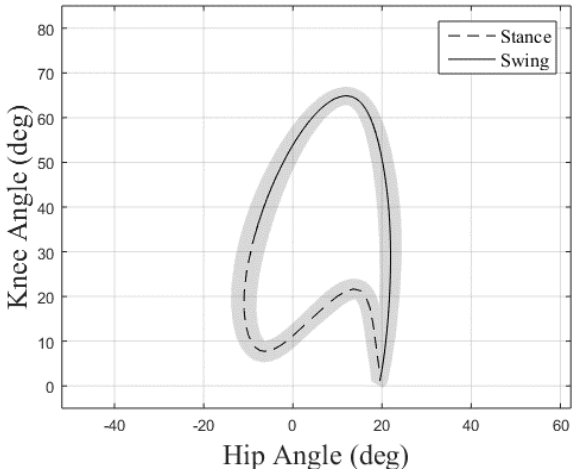


Figure 18. Example of a desired configuration path, in this case corresponding to healthy walking, as given by Winter.

At any given point in time, one particular point along the path, called $\vec{\theta}_c$, will be closest to the current configuration (in the sense of $L^2$ norm). The definition of $\vec{\theta}_c$ enables the expression of a configuration error, $\vec{e}$, as defined below:

$$\vec{e} = \vec{\theta}_c - \vec{\theta} \tag{9}$$

A local normal and tangential coordinate frame can be defined such that:

$$\hat{n} = \frac{\vec{e}}{|\vec{e}|}, \tag{10}$$

where the tangential direction is orthogonal to the normal and points in the direction of positive path traversal (clockwise in Figure 19). Figure 16 depicts the vectors described above in (7)-(10) for an arbitrary configuration and configuration time derivative.

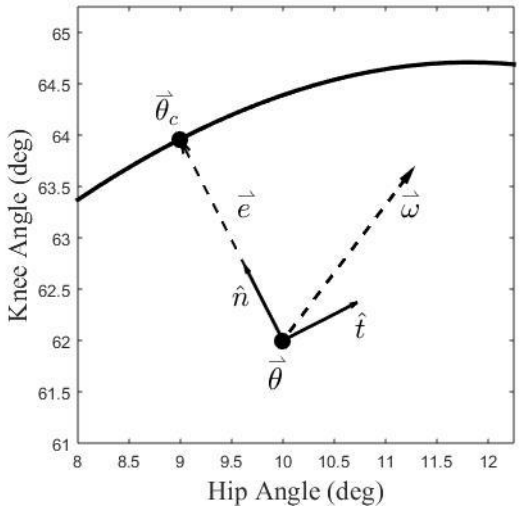


Figure 19. Conventions used to describe motion in the configuration space. Unit vectors are depicted by solid lines, other vectors are dashed lines.

### 1.3. Flow control law

In order to mitigate the issue of potential energy storage in the path control law, the authors created a control law that will not store potential energy in its homogeneous behavior. Rather than deriving the constitutive behavior of the torque vector from a potential energy field shaped according to a desired path, the control law was derived instead from a flow field shaped according to the desired path. In this case, the homogeneous (i.e., characteristic) behavior of the controller depends strictly on velocity error, and is therefore devoid of potential-type energy storage. Movement guidance is enforced through the shape of the flow field (i.e., which is an exogenous input, since the shape of the flow field is not affected by system state), while the homogeneous behavior of the control law is strictly viscous-type behavior. The authors hypothesize this approach can provide suitable movement guidance, yet will be more forgiving in the event of substantial movement deviations from the desired path, such as those potentially required to maintain balance in the event of a balance perturbation. As such, the flow controller applies corrective torques according to the following viscous flow field control law:

$$\vec{\tau}_{flow} = C_d\left(\vec{\omega}_{ref} - \vec{\omega}\right). \tag{11}$$

where (11) describes the flow force (in this case torque) on a symmetric body due to drag when immersed in a viscous fluid, where $C_d$ is equivalent to a drag coefficient, while $\vec{\omega}_{ref}$ is a flow field in the configuration space based on the desired path through it, $\vec{\theta}_c$. Written as a function of the configuration error, expressed in terms of the normal and tangential components defined previously, the flow field is given by:

$$\vec{\omega}_{ref} = \Gamma\left(|\vec{e}|\hat{n} + \frac{k_{sh}}{|\vec{e}|}\hat{t}\right) \tag{12}$$

where the scalar $\Gamma$ determines the magnitude of the velocity reference. Note that $|\vec{e}|\hat{n} + \frac{k_{sh}}{|\vec{e}|}\hat{t}$ is normalized after eq. (12) is calculated such that $\vec{\omega}_{ref}$ is a unit vector multiplied by $\Gamma$. Because it is constant, the flow field only changes direction throughout the configuration space. The assistive torque, however, does change in magnitude as the time derivative of the configuration changes. In other words, when the user is moving in the same direction and with the same velocity as the flow field, the assistive torques are zero.

The second parameter, $k_{sh}$, affects the shape of the flow field in relation to the desired path. A large $k_{sh}$ favors tangential flow and produces a flow field that mostly provides assistive torque along the path independent of the magnitude of deviation from the path. A small $k_{sh}$ favors normal flow and produces a flow field that primarily redirects the configuration back to the path for large deviations, but then provides assistance along the path when the configuration error is small.

A plot showing a nominal desired path along with streamlines for a flow field with $k_{sh}$=5, 25, and 100, respectively, is shown in Figure 20.

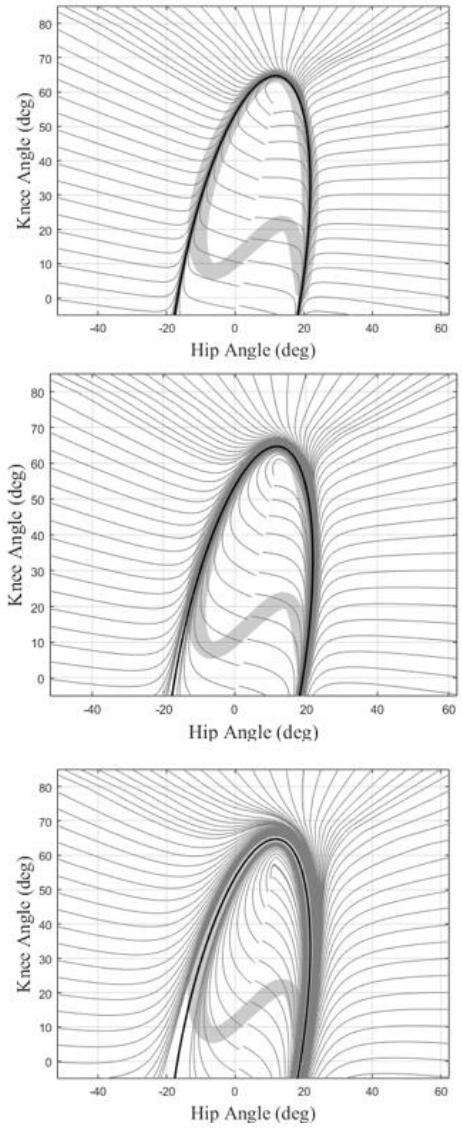


Figure 20. Streamline plot of the flow field associated with the desired swing-phase trajectory shown in Figure18. Flow field shape parameters ($k_{sh}$) for the top, middle, and bottom plots are 5, 25, and 100, respectively.

The authors note that Li and Horowitz present a control framework for contour following in robot manipulators based on a similar velocity field construct (Li and Horowitz 1999). Like the approach here, a velocity field is employed in that work because it removes the time-dependence of the desired trajectory. Rather than use the viscous flow control law (11) described here, however, the method presented by Li and Horowitz employs an augmented model-based approach that ensures passivity of the closed loop. Although that control

methodology is compelling for contour following in a robotic manipulator, the model-based methodology and associated performance objectives are not clearly transferrable to the problem described here.

## 2. Implementation and assessment

In order to assess the relative characteristics of the flow and path controllers, both were implemented on a lower-limb exoskeleton, and both tested for configuration error, and for disturbance gain, on a set of five healthy subjects, as described below.

### 2.1. Exoskeleton hardware

The controller was implemented on an open-architecture version of a commercially-available lower-limb exoskeleton (Indego Exoskeleton, Parker Hannifin Corp), shown in Figure 21. Rather than use the commercial control software, the exoskeleton was programmed with software written by the authors to implement the path and flow controllers previously described. The exoskeleton hardware platform incorporates four motors for powered movement of bilateral hip and knee joints in the sagittal plane, in addition to built-in ankle-foot-orthoses at both ankle joints to provide ankle stability and transfer the weight of the exoskeleton to the ground. Onboard electronic sensors include encoders at each joint that provide the respective joint angles and angular velocities, and six-axis IMUs in each thigh link, although the IMUs were not used in the work presented here. The total mass of the exoskeleton including the battery is 12 kg (26 lbs).


Figure 21. Photo of Indego exoskeleton

2.2. Experimental assessment protocol

Two sets of experiments were performed to comparatively assess the efficacy of the path and flow controllers. The first experiments assessed each controller's ability to provide guidance, which was assessed via average root-mean-squared (RMS) path error during swing phase. The second experiment assessed each controller's tolerance for path deviation, which was assessed by measuring the "disturbance gain," which is essentially the measured output impedance of the controller in response to large path deviations.

2.3. Experimental control gains

The path controller employs three essential gains: stiffness $k$, damping $b$, and deadband half-width $\delta$. The flow controller also employs three essential gains: field shaping gain $k_{sh}$, velocity reference magnitude $\Gamma$, and drag coefficient $C_d$. Both controllers have a trade-off between the guidance error and disturbance gain; in particular, higher control gains generally result in less guidance error, but also a larger disturbance gain. As such, an equitable comparison requires a systematic selection of control gains. In order to provide an equitable comparison in this regard, the two controllers were compared for two cases. In the first case,

gains were selected to provide similar guidance error between the two controllers, in which case the respective disturbance gains were compared. In the second case, gains were selected to provide a similar disturbance response for the two controllers, in which the respective guidance errors were compared. In both cases, the flow controller gains remained invariant, such that only the path controller gains changed, as discussed below.

As a baseline, the first path controller gain selection used the same gains previously published by the authors in a recent publication implementing the path controller on the same hardware employed here (A. Martinez, Lawson, and Goldfarb 2018). That paper found that the best path control performance, as measured by RMS path error, was achieved with the gain set listed in the first row of Table 4, which in this chapter is referred to as "path-9" since it corresponds to path control with a stiffness of 9 Nm/deg. Given this guidance performance as a baseline, flow controller gains were adjusted to provide an (approximately) matched RMS path error to the path-9 controller on a test subject. Note that the test subject was not one of the subjects employed in the experimental protocol described below. The resulting flow controller gains are given in the second row of Table 4.

Table 4. Controller parameters

| Controller | Parameter | Magnitude |
|---|---|---|
| Path-9 (from [23]) | k | 515 Nm/rad (9 Nm/deg) |
| | b | 13.0 Nm-s/rad (0.225 Nm-s/deg) |
| | $\delta$ | 0.026 rad (1.5 deg) |
| Flow | $k_{sh}$ | 16 |
| | $\Gamma$ | 2.9 rad/s (167 deg/s) |
| | $C_d$ | 0.75 Nm-s/rad (0.013 Nm-s/deg) |
| Path-3 | k | 172 Nm/rad (3 Nm/deg) |
| | b | 8.0 Nm-s/rad (0.14 Nm-s/deg) |
| | $\delta$ | 0.026 rad (1.5 deg) |

Experiments to measure the disturbance gain were conducted in addition to measuring the RMS error. In order to have a second point of comparison between the path and flow controllers, a second path controller gain selection was set to (approximately) match the disturbance gain of the flow controller on the same test subject, resulting in a set of gains listed in the third row of Table 4, which is referred to as the "path-3" controller, since the stiffness corresponds to 3 Nm/deg. Note that, for these control gains, the stiffness is a third

of the path-9 stiffness, while the damping constant was scaled by the square root of three such that that damping ratio remained invariant (for a given mass). The deadband also remained invariant. As such, two experiments were performed under three control conditions: using the path-9 controller, the flow controller, and the path-3 controller. The first experiment measured the RMS guidance error, while the second experiment measured the disturbance gain.

## 2.4. Experimental protocol

Experiments were performed on five healthy subjects (three male, two female, aged 25.8 ± 3.7 years) walking overground in the exoskeleton.

### 2.4.1. Guidance assessments

For each subject, the guidance assessment experiments consisted of six 50 m overground exoskeleton walks without a stability aid at a speed of approximately 0.8 m/s, where each controller (i.e., path-9, path-3, and flow) was used twice in a semi-random order, with the constraint that the same controller could not be presented to each subject consecutively. Each subject was required to complete the 50 m walking segment in a time of 62.5 s ± 2.5 s, which corresponds to an average walking speed between 0.77 and 0.83 m/s. If the 50 m walk time was out of this range, the data were discarded and the trial repeated later in the protocol such that the subjects did not use the same controller consecutively. A photo of a subject conducting a 50 m walk corresponding to these experiments is shown in Figure 22 (left).

### 2.4.2. Disturbance assessments

The disturbance assessment experiments consisted of overground exoskeleton walking, with the additional constraint that each subject wore a range-of-motion (ROM) limiting knee brace (Breg model T Scope Premier Post-Op) under the exoskeleton on the right leg to prevent full knee flexion. The knee brace was locked such that subjects' maximum knee flexion was limited to approximately 40 deg in the configuration space. Subjects were given a rolling walker as a stability aid for these trials. Rather than 50 m, each subject walked 25 strides using each controller (path-3, path-9, and flow) one time each, presented in a random

order. There was no attempt to regulate walking speed in these trials. A photo of a subject conducting a trial with the ROM-limiting knee brace and exoskeleton corresponding to these experiments is shown in Figure 22 (right).

Figure 22. Representative photos of Subject 2 walking in the guidance assessment trial (left) and disturbance assessment trial (right).

## 3. Data collection

During all trials, data were collected from the exoskeleton, including bilateral hip and knee angles and motor torques, at a sampling rate of 200 Hz. For all trials, the first three strides and the last two strides for each leg were not included in the results to avoid transient effects associated with the start and end of the walking trials.

### 3.1. Acclimation

Subjects were allowed to acclimate to each trial condition prior to conducting the experiments. Acclimation consisted of a minimum of four 50 m walks with the exoskeleton with no controller active (i.e., backdriving exoskeleton joints). Afterwards, subjects were required to walk a minimum of three 50 m walks using each of three controllers (i.e., path-3, path-9, and flow). Subjects could walk as many additional trials as desired, until they

confirmed that they were acclimated to all experimental conditions associated with the guidance assessments. Note that subjects were not explicitly exposed to the disturbance experimental condition (i.e., wearing the ROM-limiting knee brace) prior to that experiment.

# 4. Results

## 4.1. Overground walking tests

Figure 23 shows the respective hip and knee motion for a representative subject (in this case Subject 2), corresponding to each of the three controllers. Specifically, the data corresponds to walking with the path-3 (top left), path-9 (top right), and flow controller (bottom). Note that the right leg is shown in red; left in blue; reference path with standard deviation from (Winter 1991); swing phase in solid line; and stance phase in dashed. As shown in the plots, the path-9 and flow controllers provide similar levels of guidance, while the path-3 controller (top left) demonstrates increased guidance error.

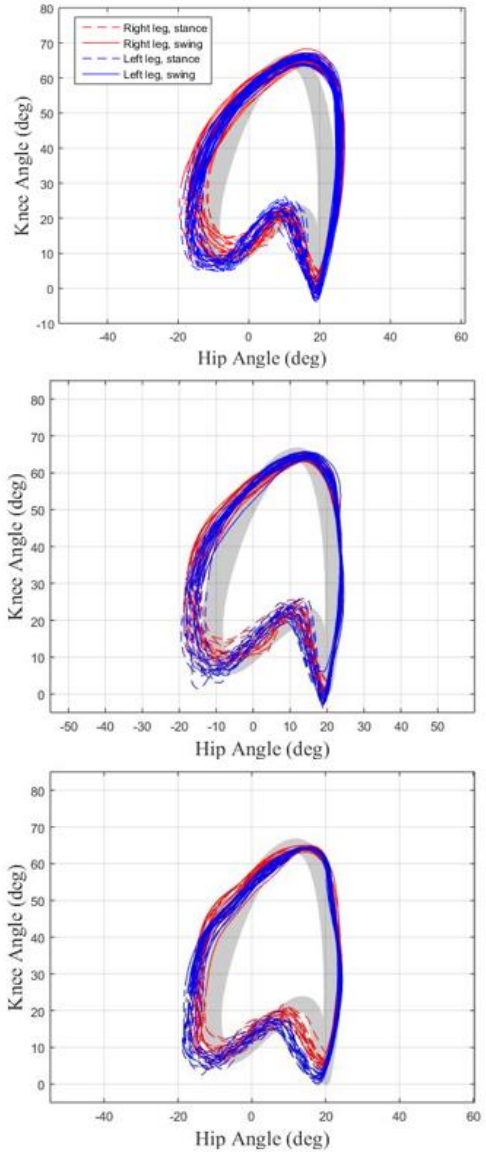


Figure 23. Representative leg motion from 50 m walking trial for the three controllers, from top to bottom: path-3, path-9, and flow. Red lines indicate right leg; blue lines left. Dashed lines represent stance phase of gait, during which (for this experiment) the respective controllers were inactive, while the solid lines represent swing phase during which the controllers were active.

The error for each trial in this chapter is given by (9), and the RMS of this error over each trial provides an indication of the efficacy of the controller in providing guidance. The mean RMS error values for all steps and all subjects for each controller is summarized in Figure 24. Specifically, for 656, 664, and 667 strides corresponding to path-3, path-9, and

flow, respectively, the average RMS error and corresponding standard deviations were 4.5 ± 2.1, 2.7 ± 1.3, and 2.6 ± 1.3 deg, respectively. Each subject's data were tested for normal distribution using a Kolmogorov-Smirnov test, and were found to be normally distributed within a 95% confidence interval (with the exception of Subject 5, path-3 data, which was found to be normally distributed with a 90% confidence interval). The differences in means of each condition for each subject were tested using repeated measures ANOVA. As such, each subject's three overground walking conditions were tested against one another. Results indicated that the differences between flow and path-3 RMS guidance errors were significant ($p<0.05$), while the differences in error between the flow and path-9 conditions were not.

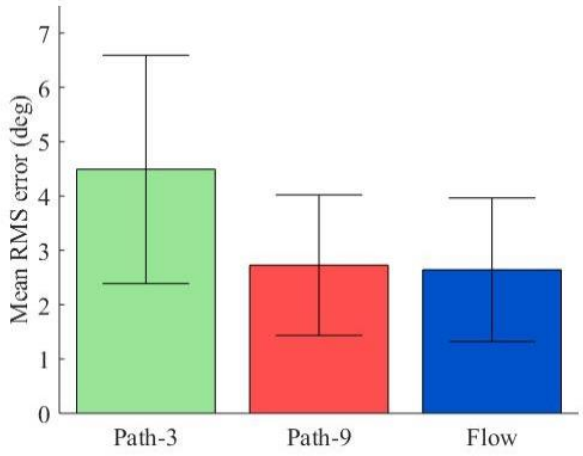


Figure 24. Mean RMS errors for the exoskeleton leg path. Error bars represent one standard deviation from the mean.

## 4.2. Disturbance response tests

Figure 25 shows hip and knee angle from the right leg from a representative subject and trial (Subject 1, path-3 controller) of the disturbance response assessment experiment.

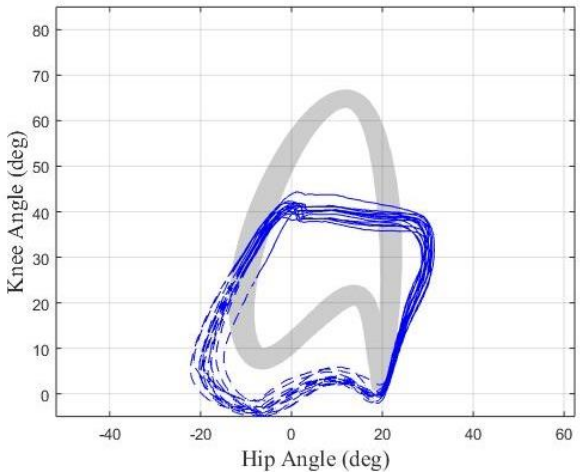


Figure 25. Representative hip and knee angle data corresponding to disturbance gain trial (i.e., exoskeleton walking while wearing ROM-limiting knee brace).

Figure 26 shows a plot of all torque versus path error samples for the all subjects and all control conditions while conducting the ROM-limiting experiments. This figure depicts the error (9) from the desired path along the x-axis, and the resulting torque from the respective controller on the y-axis, with the path-3, path-9, and flow controller data shown in green, red, and blue, respectively. A least-squares linear approximation of each set of data results in the linear parameters for each case given in Table 5. Note that the slope of each line provides the approximate disturbance gain corresponding to each controller (i.e., the torque on the user resulting from a given deviation). As shown in the table, while the path-3 and flow gains are similar (by design), the path-9 disturbance gain is approximately three times greater than that of the flow controller.

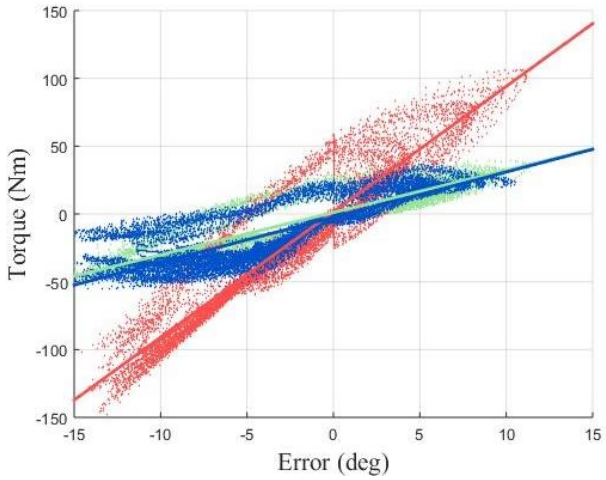


Figure 26. Torque response of each controller to deviations from the desired path for path-3 (green), path-9 (red), and flow controller (green).

Table 5. Error response linear regression coefficients

| Controller | Slope (Nm/deg) | Offset (Nm) |
|---|---|---|
| Path-3 | 3.1 | 1.1 |
| Path-9 | 9.3 | 1.6 |
| Flow | 3.3 | -2.4 |

# 5. Discussion

## 5.1. Guidance error versus disturbance gain

Recall that the intent of the flow controller is to provide effective guidance, while also allowing large deviations from a given desired path when needed without introducing large disturbance torques. In that regard, based on the results previously presented, the flow controller parameterized to provide similar guidance to a path controller was shown to provide a factor of three smaller disturbance gain; while a path controller parameterized to provide a similar disturbance gain was shown to provide (approximately) a factor of two larger guidance error.

## 5.2. Other behavioral observations of the flow controller

### 5.2.1. First-order homogeneous response

As previously mentioned, a path controller is characterized by a homogeneous position-dependence, while a flow controller is characterized by a homogeneous velocity-dependence. In the case that these control torques act on a primarily inertial leg, one would expect the path-controlled leg motion to have a nominally second-order homogeneous response, while the flow-controlled leg motion would have a first-order response. As such, one expects a flow-controlled motion to be fundamentally devoid of oscillation, while the existence of oscillation in a path-controlled leg would depend on the system parameters (i.e., on the stiffness and damping control gains, in addition to the inertial properties of the leg). It should be noted that, in the case of a leg with strong elastic-type behavior (e.g., spastic muscular tone), the exoskeleton load will be fundamentally second-order, and the viscous-dominated action of a flow controller may not have sufficient position-dependence to overcome the inherent elasticity of the leg. In such a case, a path-based approach may offer improved control authority.

### 5.2.2. Providing guidance and assistance

Recall that the control objectives for poorly-ambulatory individuals include both guidance and assistance from the exoskeleton. Guidance is defined here as facilitating or promoting a given coordination (or shape) of movement, but not otherwise directly adding power to the movement. Assistance is the complement to guidance, which is adding power along the direction of movement. In a path control approach, these two functions are generally provided via separate control mechanisms. Specifically, the path control construct is by its nature one of guidance. A path control approach is particularly compelling in this regard, since it provides guidance in a (theoretically) strictly energetically passive manner when derived from a conservative potential field and supplemented with additional damping. It is generally thought that interaction with passive machines is safer than interacting with active machines. Despite the potential for passive guidance, poorly-ambulatory individuals are often in need of assistance, in which case power must be added in the direction of motion,

thereby negating potential advantages of controller passivity. Some previously described path control approaches have employed guidance controllers based on potential energy fields, and then have supplemented them with active control components along the intended direction of movement to provide movement assistance (see, e.g., (Banala et al. 2009; Duschau-Wicke et al. 2010)). In contrast to this approach, the flow controller combines both guidance and assistance components into a single control component, as encoded by the shape of the velocity field, such that there is no mechanistic distinction between the two. Rather, the extent of guidance relative to assistance is determined by the shape of the velocity field (i.e., by the $k_{sh}$ control parameter). Note that, although not incorporated here, one can also control the relative magnitudes of guidance versus assistance torques by employing separate drag coefficients for the normal versus tangential directions defined by $\hat{n}$ and $\hat{t}$.

### 5.2.3. Directionality of error correction

An important difference between the behaviors of path and flow controllers is associated with the directionality of the corrective torques in the presence of path (or configuration) error. A path error in a path controller will always generate a corrective torque that will pull the leg normal to the path, regardless of the configuration velocity. The corrective torques generated by a flow controller, however, are dependent on both the configuration and the rate of change of configuration (i.e., the configuration velocity). In the case that a path error exists in a flow controller, if the leg is moving back towards the path with an appropriate velocity, no corrective torques will be applied, regardless of the magnitude of configuration error. In other words, the flow controller considers not only the configuration error, but also the current configuration velocity, and will not correct movement if the velocity indicates that the leg is converging toward the path. In this regard, the flow controller potentially interferes less with the user than might a path control approach.

### 5.2.4. Dependence on reference velocity

The flow controller requires selection of a reference velocity (i.e., a nominal velocity must be employed for the flow field), which in effect establishes a nominal desired step time. In the case that the user is moving along the desired configuration path at the desired velocity,

no assistive torque will be imparted. In the case that the user moves more slowly, the virtual flow field will "pull" the leg along the desired path, in a similar manner to a floating object in a stream. Similarly, if leg movement is faster than the reference velocity, the controller will impart associated drag forces to slow it. Despite the seeming dependence on this reference velocity, a flow controller is more forgiving with respect to step time deviation than would be a position-dependent assistive controller, since the latter (fundamentally) integrates velocity error over the stride, which will result in a large corrective torque for a continuous velocity error. A flow controller, on the other hand, will impose a corrective torque associated strictly with the instantaneous velocity error. As such, deviation from a nominal step time is easily achieved in practice.

Although not employed here, it is worth noting that the reference velocity could be made a function of cadence, which is similar to some previously described position-based methodologies that adjust the duration of a swing-phase trajectory based on a measure of cadence.

## 6. Conclusion

This chapter describes a controller for a lower limb exoskeleton that addresses the need to provide movement guidance and assistance to the lower limbs. The controller allows for deviations from the desired motion without introducing large disturbance torques. The controller approach mimics the effect of the viscous forces on a uniform object in a flow field, and therefore is called a flow controller. The ability of the flow controller to provide movement guidance, and the ability of the controller to tolerate deviation from that guidance were compared to a previously-published guidance controller in experiments on five healthy subjects. The experimental results indicate that the flow controller was able to effectively guide leg movement while offering less resistance to large path deviations.

# CHAPTER V

# SINGLE DEGREE OF FREEDOM FLOW CONTROLLER

There are many individuals with lower limb movement impairment who require or may benefit from walking assistance. Common causes of movement impairment include stroke, incomplete spinal cord injury (iSCI), multiple sclerosis (MS), and cerebral palsy (CP). Individuals who have movement impairment, but are still capable of ambulation, are herein referred to as poorly-ambulatory individuals. Poorly-ambulatory individuals' leg movements are typically characterized by leg muscle weakness and potentially also by spastic muscle tone. Common assistive devices for these individuals include quad canes and ankle-foot orthoses (AFOs).

In recent years, powered assistive devices (herein referred to as powered exoskeletons) have emerged as an option to replace or supplement traditional (passive) assistive devices (Yan et al. 2015; A.J. Young and Ferris 2017; Meng et al. 2015; Chen et al. 2013). The nature of the design and control of a given powered exoskeleton is highly dependent on the nature of the impairment and needs of the individual who will use it. In this work, the authors focus on applications in which subjects can benefit from single-joint assistance – specifically powered assistance at the knee. For this application, the authors seek an exoskeleton and control approach that provides movement guidance and assistance at the knee during swing phase and support during stance phase, yet does not dictate step (or trajectory) time and is forgiving to deviations in desired movement.

Various exoskeleton controllers for walking assistance have been presented and discussed in the literature, including torque-pulse (or oscillator-based) controllers (Arazpour et al. 2016; Garate et al. 2017; Murray et al. 2015; Ronsse et al. 2011; Bae et al. 2015; Lerner, Damiano, and Bulea 2017; Ward et al. 2012; Quinlivan et al. 2017; De la Fuente, Sugar, and Redkar 2017; Sugar et al. 2015), potential-energy-based approaches that provide a virtual tunnel or path to guide movement (Banala et al. 2009; Duschau-Wicke et al. 2010; A. Martinez, Lawson, and Goldfarb 2018), and trajectory-based controllers (Suzuki et al. 2007; Neuhaus et al. 2011; Quintero, Farris, and Goldfarb 2012; S. Wang et al. 2015; Bortole et al. 2015; Esquenazi et al. 2012; Hartigan et al. 2015; Kozlowski, Bryce, and Dijkers 2015). In

a previous publication, the authors describe a “flow controller,” which is a form of exoskeleton control that provides desirable control characteristics relative to the previously stated control objectives (i.e., movement guidance and assistance without time constraints and with tolerance for movement deviation). The flow controller, however, was constructed as a fundamentally multi degree-of-actuation (mDOA) controller (i.e., its formulation is based on a configuration space of two or greater). The application of interest herein is a multi-degree-of-freedom (mDOF) but single DOA (sDOA) application. Specifically, the controller is intended to support a given movement coordination between the hip joint and knee joint during swing phase (hence mDOF), but only the knee joint is actuated (hence sDOA). This type of system is referred to here as an mDOF/sDOA application.

Since the previously presented flow controller provides the control and interaction characteristics sought in this application, the authors sought to modify the previously-presented flow controller for this mDOF/sDOA application, and to investigate the extent to which this approach provides effective control for such applications. As such, the modified flow controller was implemented on a knee exoskeleton prototype, and the controller and exoskeleton tested on two individuals with hemiparesis from stroke, specifically to assess the extent to which the exoskeleton and controller improve knee movement and hip/knee coordination during walking.

## 1. Flow Controller for mDOF/sDOA application

The controller provides three distinct behaviors in different phases of gait. During swing phase, the knee exoskeleton is intended to provide movement guidance and assistance that coordinates hip and knee motion. During early and middle stance phase, the exoskeleton is intended to provide knee support, while during late stance phase the exoskeleton removes knee support to allow the user to initiate swing phase. The controller is moved between these difference gait phases by a finite state machine, which is comprised of three corresponding states: swing, stance, and late stance. The flow controller, which provides guidance and assistance during swing phase, is active only in the swing state.

### 1.1. Sensing Requirements

The flow controller is constructed within a multi DOF configuration space. In its previously presented form, the flow controller was presented in a two DOF configuration space comprised of hip and knee angle. Since hip angle is not measured in the knee exoskeleton application considered here, the configuration space is instead described in terms of thigh angle (relative to the vertical) and knee angle. The knee exoskeleton described here also includes foot/floor force sensing, which is employed to facilitate state detection. As such, the controller described here requires real-time sagittal-plane thigh angle (relative to the vertical) and angular velocity measurement, knee angle and angular velocity measurement, and foot/floor force detection. The implementation of this sensing is discussed in more detail in the implementation section.

### 1.2. State Machine

The swing, stance, and late stance behaviors are selected by the state machine depicted in Figure 27. The conditions for switching between the states are based on the thigh angular velocity ($\omega_{th}$) for the toe off state transition and the heel force detection ($F_{heel}$) from loading at the heel strike. The thigh angle, and knee angle readings ($\theta_{th}$ and $\theta_k$, respectively) act as a guard condition for false positives for the transition into swing phase. The joint convention for the thigh segment angle and angular velocity indicates that extension is positive, while flexion is negative. Knee joint angle convention is positive in extension and negative in flexion. Note that the knee angle guard condition was adjusted for each subject's individual gait, as seen in Table 8.

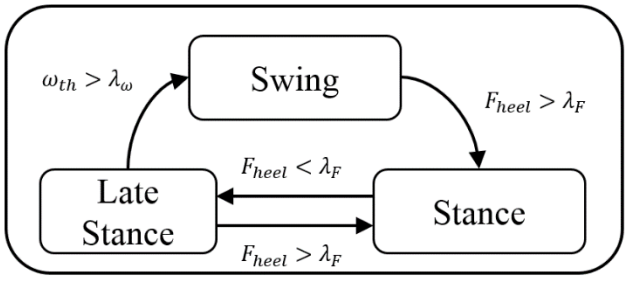


Figure 27. Controller state machine diagram. Transition values are: $\omega_{th} > 0$ deg/s; $F_{heel} > 25$ N.

### 1.3. Stance Phase Control

The stance phase controller remains the same form as described in (Andres Martinez et al. 2018). The controller supports the user in knee extension when the leg is on the ground (i.e., $F_{heel}$ > 25 N). Note the heel contact force reading was low-pass filtered at 20 Hz. Additionally, the heel contact force readings changed from 5 N in swing phase to over 400 N in stance phase depending on subject weight. The stance controller is composed of a virtual unidirectional stiffness around an equilibrium point of $\theta_k = 0$ that assists the user only in extension. The stiffness and damping values employed in the subsequent implementation are listed in Table 9.

### 1.4. Swing Phase Flow Control

The objective of swing phase control is to facilitate movement coordination without dictating step time, in a manner that is forgiving to deviation from the desired movement. The flow control approach provides these control objectives, but was previously formulated within a multi DOA configuration space. This chapter examines the extent to which this approach might provide suitable control of swing-phase in a single DOA application, specifically for a powered knee exoskeleton. In order to examine this, the previously-presented flow controller was modified in three ways: 1) thigh motion was substituted for hip motion in the configuration space; 2) the flow field was constructed differently to eliminate discontinuities in the flow field within the allowable range of motion; and 3) only the knee component of control torque was utilized in the controller.

The configuration space for this modified version of the flow controller is given by the vector:

$$\vec{\theta} = (\theta_{th}, \theta_k), \tag{13}$$

where $\theta_{th}$ and $\theta_k$ are the thigh and knee joint angles, respectively, and the vector $\vec{\theta}$ is referred to as the configuration. The time derivative of the configuration is given by:

$$\vec{\omega} = \frac{d\vec{\theta}}{dt}. \tag{14}$$

The desired movement is defined as a relationship between $\theta_{th}$ and $\theta_k$ in the

configuration space. Although it can be described by any desired path, an ellipse centered at the origin provides a good approximation of the relationship observed during healthy walking:

$$\frac{{\theta_k}^2}{a^2} + \frac{{\theta_{th}}^2}{b^2} = 1. \quad (15)$$

Note that a slight forward tilt to the ellipse is a somewhat better description of healthy movement, but sufficiently slight that the authors employed (15) instead for this investigation.

The flow control action is defined relative to a flow field, which is defined relative to the desired movement (15). In this chapter, the desired flow field is defined differently from the flow field described in the previous chapter. In that work, the flow field was defined relative to the normal from the desired path. Although that construction was effective in that implementation, it was somewhat deficient in that application, and particularly deficient in this application. Specifically, in the flow field construction described in chapter VI, a portion of the flow field some distance from the desired path was discontinuous along the major axis of the ellipse. In that case, in the implementation described, the flow field discontinuity was far from the desired path, and since the configuration space was fully actuated, the exoskeleton was able to keep the actual movement close to the desired path and away from the flow field discontinuity. As such, the flow field was deficient (i.e., contained a discontinuity in the configuration space), but the deficiency was not observed. In the case considered here, however, the thigh angle configuration is an unactuated DOF, and as such, the controller has no capacity to keep the thigh DOF near the desired path. Thus, the movement in this application is less constrained to a given part of the configuration space, and as such, the flow field should be devoid of discontinuities within the achievable range of motion. The flow field was therefore redefined in this chapter such that a singular flow field discontinuity would exist at the edge of the range of motion (i.e., when the knee is fully extended), so that a user would not be expected to cross this discontinuity during swing phase. The modified flow field is constructed as follows. A configuration vector can be defined by the slope $m$ from the origin $\theta_0 = (0,0)$, $\theta_k = m\theta_{th}$, which can be rearranged to:

$$\theta_{th} = \frac{\theta_k}{m}. \quad (16)$$

The knee angle at the intersection with the desired movement can be found by combining eq. (16) and eq. (15) and using the solution $\theta_{k,ell} > 0$, as the knee angle is always positive in this convention, as seen in Figure 28. The corresponding $\theta_{th}$ can be found by plugging the result into eq. (16).

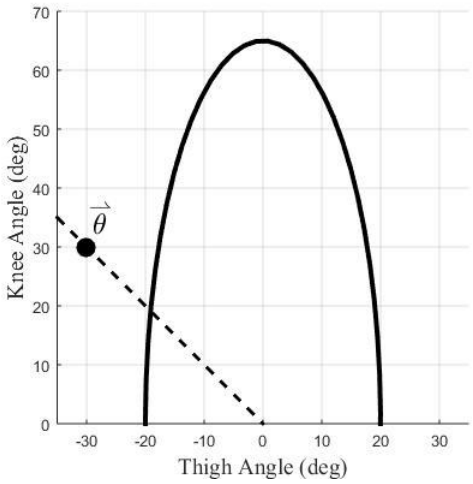


Figure 28. Plot of a desired path defined in eq. (15) as an ellipse and the line from the origin to the configuration $\vec{\theta}$ as defined in eq. (16).

The tangent lines to the ellipse at the point of intersection, $\theta_{ell} = (\theta_{h,ell}, \theta_{k,ell})$, are the basis for the direction of the flow field, as seen in Figure 29. The tangent vector can be found by differentiating eq. (15) with respect to $\theta_{th}$:

$$\frac{d\theta_k}{d\theta_{th}} = -\frac{a^2}{b^2}\left(\frac{\theta_{th,ell}}{\theta_{k,ell}}\right). \tag{17}$$

The tangent angle from the horizontal axis can be found using the four-quadrant inverse tangent:

$$\alpha_{tan} = atan2(d\theta_k, d\theta_{th}). \tag{18}$$

The flow field is created by finding the radial distance from the current configuration to the intersection:

$$e_{ell} = \sqrt{({\theta_{th,ell}}^2 - {\theta_{th,l}}^2) + ({\theta_{k,ell}}^2 - {\theta_{k,l}}^2)}. \tag{19}$$

Given the angle of the tangent line with respect to the horizontal axis, the angle of the flow lines can be found:

$$\alpha_{flow} = \alpha_{tan} + \text{atan}\left(\frac{e_{ell}}{k_{sh}}\right). \tag{20}$$

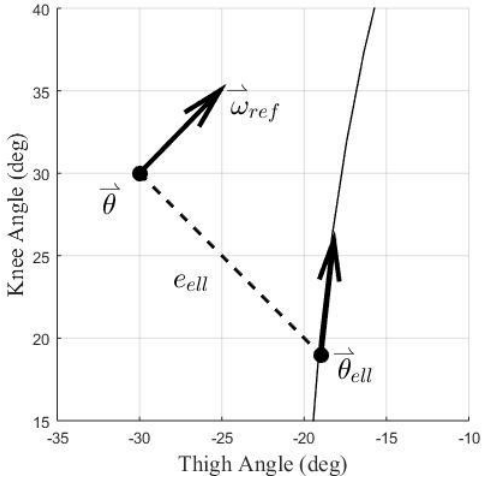


Figure 29. Representation of the reference velocity as defined in eq. (23) in configuration space. The flow vector direction is calculated from the tangent line path given by eq. (18), and adjusted by the magnitude of the error to the desired path $e_{ell}$, as given in eq. (19).

In this construction, the parameter $k_{sh}$ affects the shape of the flow field in relation to the desired path. A large $k_{sh}$ favors tangential flow and produces a flow field that mostly provides assistive torque along the path independent of the magnitude of deviation from the path. A small $k_{sh}$ favors normal flow and produces a flow field that primarily redirects the configuration back to the path for large deviations, and provides assistance along the path only when the configuration error is small. Figure 30 shows the desired path of leg travel imposed by the flow controller at any point in configuration space.

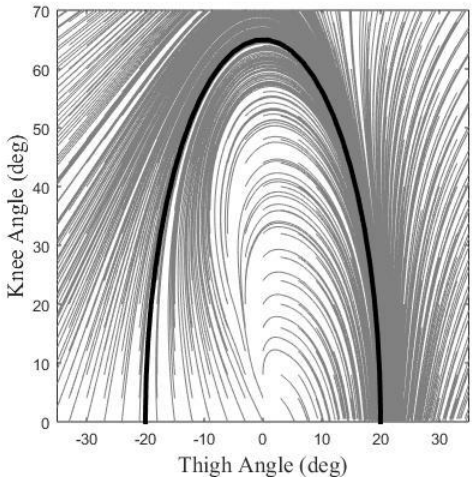


Figure 30. Streamline plot of the flow field associated with the desired swing-phase trajectory shown in Figure 28 with $k_{sh} = 50$.

The flow field unit vectors that define the configuration are given by:

$$\hat{f} = \cos(\alpha_{flow})\,\hat{\imath} + \sin(\alpha_{flow})\hat{\jmath}. \tag{21}$$

and the reference velocity is:

$$\vec{\omega}_{ref} = \Gamma \hat{f}, \tag{22}$$

where the scalar $\Gamma$ determines the magnitude of the velocity reference. The flow controller applies corrective torques according to the following viscous flow field control law:

$$\vec{\tau}_{flow} = C_d(\vec{\omega}_{ref} - \vec{\omega}). \tag{23}$$

where (23) describes the flow force (in this case torque) on a symmetric body due to drag when immersed in a viscous fluid, where $C_d$ is equivalent to a drag coefficient, while $\vec{\omega}_{ref}$ is a flow field in the configuration space based on the desired path through it as detailed in eq. (15).

Recall that the controller outlines a desired path of travel in configuration space, eq. (15). When implemented on a powered knee exoskeleton, as described in this chapter, the knee torque is a function of both thigh and knee movement, but only the knee is affected by the control action.

### 1.5. Walking detection

The controller detects whether the user is walking or standing by measuring the foot-floor force readings, thigh angle, and thigh angular velocity. Walking is detected when all of the following conditions are met:

$$\begin{cases} F_{heel} < \lambda_F \\ \theta_{th} < \lambda_\theta \\ \omega_{th} > \lambda_\omega \end{cases}. \tag{23}$$

These thresholds are listed for the implementation here in Table 10. If any of the three thresholds are not met over three seconds after transitioning from swing phase to stance phase, the controller reverts to the standing state. The stand-to-walk detection prevents the user from triggering false positive transitions from stance phase to swing phase when shifting weight during standing.

## 2. Controller Implementation and Assessment

In order to assess the controller performance relative to daily use devices, the controller was implemented on a knee exoskeleton. The controller was tested for knee kinematics, user symmetry while walking, user walking speed, and controller torque outputs. Experiments were conducted on two individuals with hemiparesis following stroke.

### 2.1. Exoskeleton Hardware

The controller was implemented on the knee exoskeleton prototype shown in Figure 31. The knee exoskeleton is essentially a standard knee-ankle-foot orthosis (KAFO) with a powered knee module in place of a standard knee joint. The ankle joint, which is standard, is an articulated joint with adjustable dorsiflexion and plantarflexion range-of-motion limits. The thigh segment of the exoskeleton is supported by bilateral uprights. The knee joint on the medial aspect is a standard passive hinge joint, while the knee joint on the lateral aspect is a custom actuated knee joint. The actuated knee joint is driven by brushless motor (Maxon EC-52i) and two-state chain-drive transmission, which is packaged separately from the knee joint and located on the lateral aspect of the thigh, and actuates the knee joint remotely

through a pair of Bowden cables. The actuation unit is capable of maximum continuous torque of 15 Nm and peak torque of 20 Nm. The actuation unit is powered by a lithium ion battery pack consisting of six 18650 cells (INR18650-30Q) in series, providing nominal 25.2 V and 72 W-hrs at full charge, with a maximum continuous current capacity of 15 A. The battery pack has a mass, including housing, of 355 g. The total mass of the knee exoskeleton including the actuation cassette, KAFO structure, and battery is 2.0 kg.

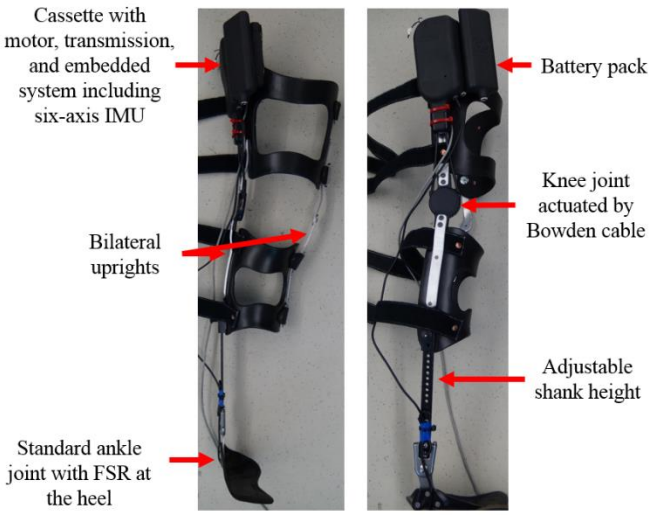


Figure 31. Photos of the knee exoskeleton from the front view (left) and side view (right).

Sensing includes encoders in the knee actuation cassette which measure knee angle and angular velocity, a six-axis IMU that provides thigh angle and angular velocity measurement, and a FSR located on the bottom of the AFO for ground force measurement. The actuation unit includes an embedded system that runs a low-level control, including brushless motor current control, and also includes a CAN interface that enables high-level control prototyping and data collection from a laptop computer via the real-time interface provided by MATLAB/Simulink at a sampling rate of 500 Hz.

Recall that real-time sagittal-plane measurement of thigh angle is required for the swing-phase controller. This measurement is provided using a combination of measurement techniques. During stance phase, the thigh angle is calculated via a standard complementary filter sensor fusion that combines a low-pass-filtered estimate based on sagittal-plane accelerations with an integrated and high-pass-filtered estimate based on the sagittal-plane

gyroscope, with the low and high-pass filter cutoffs set to 0.16 Hz. In order to provide a faster estimate during swing phase, an initial thigh angle is determined from the complementary filter at toe-off detection, after which the thigh angle for the remainder of swing phase is estimated using a pure integration of the gyroscope. Once swing phase ends, the thigh angle is again estimated using the complementary filter.

### 2.2. Experimental Protocol

Experiments were performed on two subjects with hemiparesis following stroke. Subject information including age, time since last stroke incident, paretic side, and daily use assistive devices are shown in Table 6. The extent of muscle spasticity in each subject's paretic leg is characterized by the Modified Ashworth Scale (MAS), listed for each subject in Table 7. The experimental procedure involving human subjects in this chapter was approved by Vanderbilt University's Institutional Review Board.

The controller's ability to influence a subject's paretic leg during overground walking was assessed in self-selected, single speed, 50-meter walking tests. Subjects walked in two conditions: a control walk with their daily use devices (if any), and with the exoskeleton using the flow controller.

Experiments with each subject occurred over the course of two sessions, each on a different day: a first session for fitting, calibration, and acclimation, and a second session for data collection.

During the first session, each subject was fitted to the device and familiarized with the stance phase state. The remainder of the session was used to calibrate the controller's state transitions to level ground walking.

During the second session, subjects walked several trial walks, where each trial consisted of a 50 m walk at a self-selected speed. The trial walks were performed under two conditions: one without the knee exoskeleton, but with any daily-use assistive devices (hereafter called "control walks"), and one with the knee exoskeleton (hereafter called "exoskeleton walks"). Trials were performed in the following order: two control walks, four exoskeleton walks, and two additional control walks. During these trials, walking speed was recorded using a stopwatch to measure the time taken to walk 30 meters (between 10 meter and 40 meter marks). Figure 32 shows Subject 1 walking with the knee exoskeleton.

An additional test was conducted with the exoskeleton to assess ability to step up and down curbs, and particularly the extent to which the exoskeleton allowed or interfered with this task. In these trials, subjects stepped up onto and subsequently down from a 10.5 cm tall, 183 cm long curb.

Table 6. Subject information

| Subject | Age (years) | Time since stroke (years) | Paretic leg | Daily use assistive devices |
|---|---|---|---|---|
| 1 | 37 | 7 | Right | Cane |
| 2 | 52 | 9 | Left | None |

Table 7. Subject Modified Ashworth Scales

| Subject | Parameter | Score (out of 4) |
|---|---|---|
| 1 | Hip flexors/extensors | 0 |
| | Knee extensors | 1+ |
| | Knee flexors | 1+ |
| | Ankle plantar flexors | 2 |
| 2 | Hip flexors/extensors | 0 |
| | Knee extensors | 0 |
| | Knee flexors | 1 |
| | Ankle plantar flexors | 1 |

## 2.3. Controller Parameters

The controller parameters used in the testing are listed in Tables 8 through 11. For the state controller, all thresholds were uniform between subjects, except the knee angle threshold to transition to swing. Specifically, the knee angle threshold for Subject 2 was lowered to 1 deg, to accommodate difficulty flexing his knee to initiate swing.

The flow controller employs three essential gains: field shaping gain $k_{sh}$, velocity reference magnitude $\Gamma$, and drag coefficient $C_d$. The shaping gain was the same for all subjects at $k_{sh}$=50 to maintain consistency across trials during the experimental protocol. The velocity reference magnitude $\Gamma$ describes a nominal movement velocity for the user's leg. The value of $\Gamma$ was varied between subjects to adjust for their preferred walking speed. Note that this value could be made cadence-dependent, but was not done so for the testing

described here. The drag coefficient $C_d$ is essentially the gain between velocity error and joint torque, and therefore is directly associated with the strength of the corrective torques. The drag coefficient was separated into flexion and extension ($C_{d,flex}$ and $C_{d,ext}$, respectively) drag coefficients to better assist users who are better assisted with asymmetric assistance in either direction during swing phase.

Table 8. Controller state transition parameter thresholds

| Subject | Parameter | Threshold |
|---|---|---|
| 1 | $\lambda_k$ | 15 deg |
| 2 | $\lambda_k$ | 1 deg |
| 1, 2 | $\omega_{th}$ | 0 deg/s |
| 1, 2 | $F_{heel}$ | 25 N |

Table 9. Stance phase controller gains

| Gain | Magnitude |
|---|---|
| Stiffness | 2 N/deg |
| Damping | 0.002 N-s/deg |

Table 10. Walking detection threshold

| Threshold | Magnitude |
|---|---|
| $F_{heel}$ | 25 N |
| $\theta_{th}$ | -5 deg |
| $\omega_{th}$ | 75 deg/s |

The flow controller gains employed for each subject are given in Table 11.

Table 11. Experimental control gains

| Subject | Parameter | Magnitude |
|---|---|---|
| 1 | $\Gamma$ | 600 deg/s |
| | $C_{d,flex}$ | 0.040 Nm-s/deg |
| | $C_{d,ext}$ | 0.013 Nm-s/deg |
| 2 | $\Gamma$ | 700 deg/s |
| | $C_{d,flex}$ | 0.020 Nm-s/deg |
| | $C_{d,ext}$ | 0.013 Nm-s/deg |

## 2.4. Data Collection

Knee angle and motor torque data from the knee exoskeleton were collected at a sampling rate of 1000 Hz. The first five and last three strides were not included in the results to avoid transient effects associated with stand-to-walk and walk-to-stand transitions.

An IMU-based motion capture system (Xsens AWINDA) was used to measure lower limb joint angles during overground walking. A lower limb skeletal model was created for each subject using the Xsens MVN 2018 software. Seven IMUs were placed on each subject: one on the lower back over the subject's sacrum; three on each leg, and one at the foot. The skeletal model was calibrated at the start of each set of trials (i.e., prior to the first two control walks; prior to the exoskeleton walks; and prior to the last two control walks). Motion capture data from the Xsens system was recorded at 100 Hz. Following data collection, the data were parsed into individual strides based on the state machine transition from swing to stance, and each stride was then normalized to a stride percentage.

Figure 32. Photo of subject 1 walking while using the powered exoskeleton.

3. Results

Figures 33 through 35 show respectively the measured movement for all steps in the configuration space for Subjects 1 and 2 walking without the exoskeleton (top, blue) and with the exoskeleton (middle, red), in addition to the mean movement for both cases plotted together (bottom). Note that each case is comprised of between 95 and 115 strides.

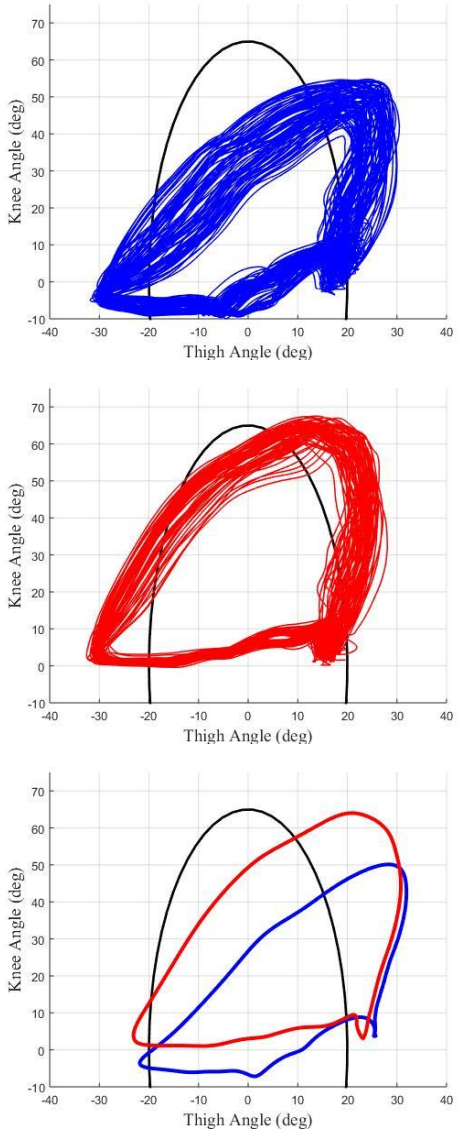


Figure 33. Thigh and knee angles during walking for subject 1 as recorded by the Xsens motion capture system. Plots show all steps without exoskeleton (top); all steps with exoskeleton (middle); and mean paths for both cases (bottom).

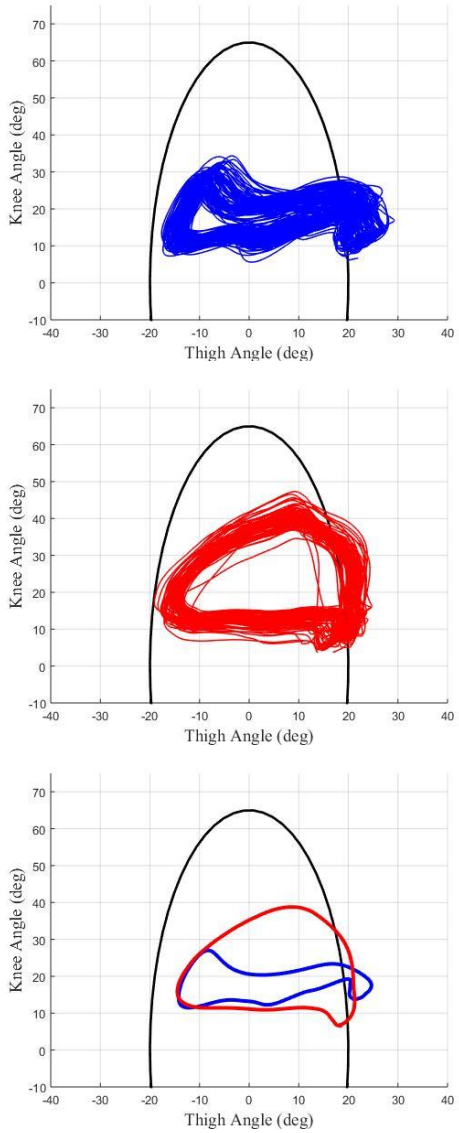


Figure 34. Thigh and knee angles during walking for subject 2 as recorded by the Xsens motion capture system. Plots show all steps without exoskeleton (top); all steps with exoskeleton (middle); and mean paths for both cases (bottom).

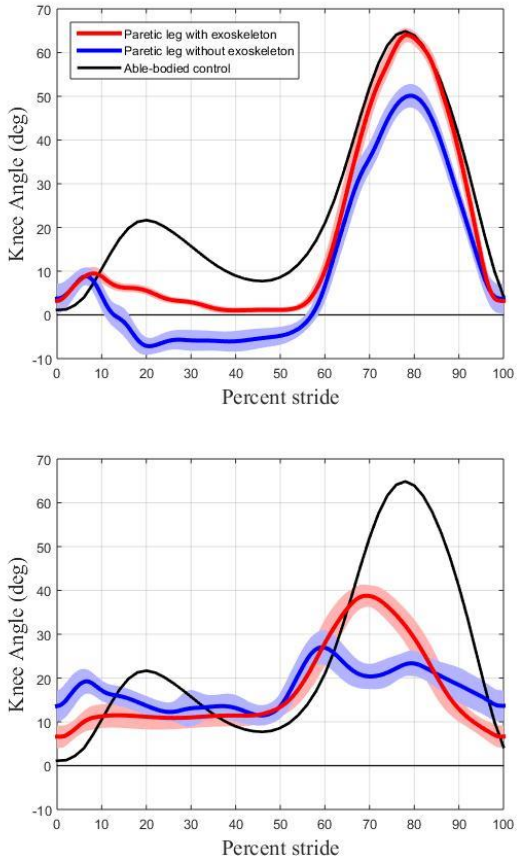


Figure 35. Subject knee kinematics as measured by the Xsens motion capture system. Subjects 1 and 2 are depicted at the top and bottom plots, respectively. Red lines indicate kinematics of the trials with the knee exoskeleton); blue lines indicate control trial kinematics (without the knee exoskeleton). The shaded blue and red represent ±1 standard deviation from the mean. The black line shows able-bodied control data (Winter 1991).

The mean knee torque applied to each subject by the exoskeleton as a function of percent stride, corresponding to the data in Figures 33-35, is shown in Figure 36. Positive torques indicate flexion torques at the knee, whereas negative torques indicate extension.

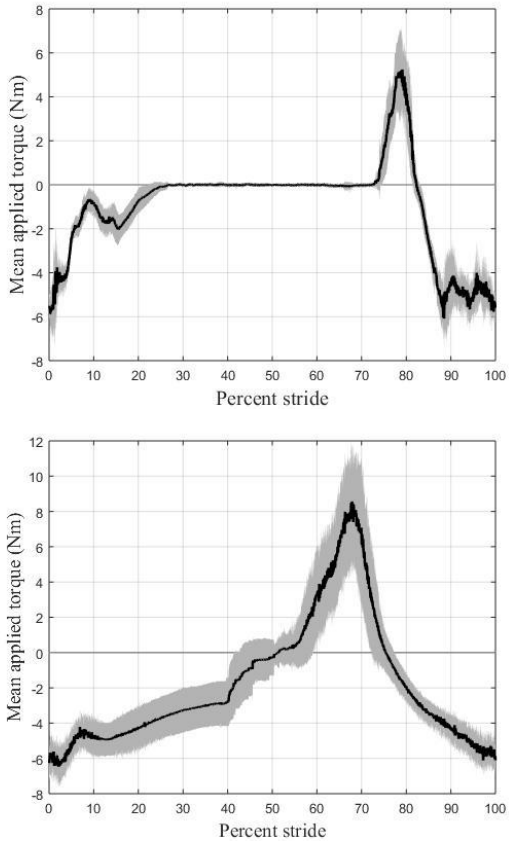


Figure 36. Torques applied to subjects' paretic leg as a function of percent stride. Subjects 1 and 2 are shown at the top and bottom, respectively. Positive torques indicate flexion torques at the knee, whereas negative torques indicate extension. The grey outline represents ±1 standard deviation from the mean.

## 4. Discussion

Recall the intent of this chapter was to examine the extent to which the flow controller provides appropriate assistance during walking in a mDOF/sDOA system, particularly for a powered knee exoskeleton; namely, the extent to which it provides guidance while also being forgiving to deviations from a desired movement.

### 4.1. Swing phase behavior

The flow controller was able to substantially increase swing-phase knee flexion for all subjects. As subsequently discussed, the ability of the controller to do so was primarily limited by a combination of each subject's muscle tone (i.e., extent of spasticity) and their comfort (i.e., how much active knee torque they were comfortable with). For all subjects,

peak knee flexion was increased substantially during swing phase. Specifically, for Subject 1, the knee exoskeleton and sDOA flow controller increased peak knee flexion by 13 deg, to an approximate healthy level. For Subject 2, the knee exoskeleton increased peak knee flexion by 19 deg. Note that, although the exoskeleton improved knee flexion for Subject 2, the resulting knee flexion is still well short of healthy knee flexion, due to the fact that Subject 2 has considerable spastic tone, as subsequently discussed.

### 4.2. Stance phase behavior

The knee exoskeleton also improved stance knee behavior for all subjects, although in different capacities. Subject 1's walking without the exoskeleton was characterized by knee hyperextension during stance phase, which was eliminated when using the exoskeleton. This is apparent in the data shown in Figure 35. Subject 2's walking without the exoskeleton was characterized by greater than normal knee flexion, which was reduced when wearing the exoskeleton. This is also apparent in Figure 35.

### 4.3. Limitations in controller performance

The extent to which the exoskeleton can influence knee kinematics of an individual with hemiparesis (Figure 35) is substantially affected by muscle spasticity in the paretic leg, as characterized by their respective MAS scores (Table 11). MAS scores indicate resistance to involuntary movements; they do not indicate the user's joint functionality due to volitional movements or range of motion. An MAS score of 0 indicates the subject has no increase in muscle tone with movement, as expected in a healthy individual; MAS of 1 indicates a slight increase in resistance; 1+ indicates a slight increase in resistance with a substantial increase at some point in the range of motion; and an MAS of 2 or greater indicates a marked increase in tone with movement.

As given in Table 11, although Subject 1 was characterized by a relatively low amount of spasticity, Subject 2 was characterized by an MAS of 1+ in both knee flexion and extension. Subject 2, in particular, started to exhibit a marked increase in passive resistance at a knee flexion angle of approximately 40 deg. Although the exoskeleton is capable of providing more torque than the nominal 8 Nm delivered to Subject 2 during swing phase,

the subject was not comfortable with higher levels of assistive torque. In this particular case, the knee exoskeleton appears to improve walking, despite the higher levels of spastic tone. One can assume, however, that the exoskeleton is best suited for individuals with MAS between 0 and 1; potentially suited to individuals with MAS of 1+; and most likely not suited to individuals with MAS at or above 2.

Subject comfort was an important criterion for the authors, as a subject who is comfortable using a device is more likely to adopt the device for daily use. The controller gains (and subsequent output torques) were tuned using subjects' verbal feedback. The drag coefficient ($C_d$) was started at a 0.005 Nm-s/deg for both flexion and extension and the velocity reference magnitude ($\Gamma$) was started at 400 deg/s. The velocity reference magnitude was increased to adjust for subjects' walking speed and the drag coefficient was increased during the acclimation session until subjects indicated that they did not want additional flexion or extension torques. Table 9 shows the final experimental control gains used by the subjects. Note that the stance phase controller remained identical for all subjects. The flow control gains resulted in applied peak torques of 6 to 8 Nm, despite the powered knee exoskeleton being able to apply approximately 20 Nm peak torque. Although increasing gains would increase the control authority, the subjects tested in this chapter preferred a balance between comfort and assistance (i.e., preferred a lower than maximum control authority).

Subjects were asked for their opinion of the controller during overground walking. Subject 1 stated that the powered knee exoskeleton allowed for more consistency during overground walking, specifically referring to paretic leg heel strike and the knee support applied in early stance (as demonstrated by Figure 35 with the standard deviation during stance phase). Subject 2 mentioned that the powered knee exoskeleton was helpful for flexion assistance (as evidenced by Figure 36), and felt comfortable while walking and wearing the device.

## 5. Conclusion

This chapter describes the application of a flow controller to a single DOA application, namely a powered knee exoskeleton. A modified version of the flow controller was developed and implemented in a powered knee exoskeleton. The exoskeleton and controller

were tested on two poorly-ambulatory subjects with hemiparesis from stroke, and shown to improve both swing-phase and stance-phase movement during walking.

# CHAPTER VI

# CONCLUSION

This document details the design and subsequent implementation of control methodologies for powered lower-limb orthosis for individuals with ambulatory disabilities. Through the chapters, the major contributions of this work are summarized sequentially as follows:

1. Adaptation of an existing path-based controller for use in overground walking with a powered lower-limb orthosis. The path controller was assessed for its ability to guide the user's legs while allowing for step time and length variability. The controller, however, was limited because it does not provide assistance to complete swing phase during walking and was unforgiving to deviations to the desired path of leg travel. As a result, a new controller was developed.
2. The design of a velocity-field-based 'flow' controller. The flow controller was shown to be an improvement over the path-based controller in its ability to provide assistance and guidance to the user's legs while being forgiving to deviations from the desired path of leg travel.
3. Adapting the flow controller for a single degree of freedom. Many individuals could potentially benefit from a single DOF exoskeleton. The flow controller possesses desirable properties for this application, but it was not clear how well it reduces to a single degree of actuation. In order to investigate the efficacy of the flow controller for a single DOA system, the flow controller was adapted for use on a knee-ankle-foot orthosis with a powered knee and tested on two individuals with hemiparesis following stroke. The controller was able to successfully improve subjects' knee kinematics on subjects who had weakness in flexion or extension.

Future research should investigate which individuals are best suited to use the flow controller. This research would involve further testing on individuals with hemiparesis from

stroke to better gauge the tone and ambulatory ability to which the flow controller is best suited. Further, the flow controller can be investigated on individuals with bilateral movement disabilities such as incomplete spinal cord injury, multiple sclerosis, cerebral palsy, and post-polio syndrome.

# REFERENCES


Aoyagi, Daisuke, Wade E. Ichinose, Susan J. Harkema, David J. Reinkensmeyer, and James E. Bobrow. 2007. "A Robot and Control Algorithm That Can Synchronously Assist in Naturalistic Motion during Body-Weight-Supported Gait Training Following Neurologic Injury." *IEEE Transactions on Neural Systems and Rehabilitation Engineering* 15 (1): 387–400. https://doi.org/10.1109/TNSRE.2007.903922.

Arazpour, Mokhtar, Alireza Moradi, Mohammad Samadian, Mahmood Bahramizadeh, Mahmoud Joghtaei, Monireh Ahmadi Bani, Stephen W Hutchins, and Mohammad A Mardani. 2016. "The Influence of a Powered Knee–Ankle–Foot Orthosis on Walking in Poliomyelitis Subjects: A Pilot Study." *Prosthetics and Orthotics International* 40 (3): 377–83. https://doi.org/10.1177/0309364615592703.

Bae, Jaehyun, Stefano Marco Maria De Rossi, Kathleen O'Donnell, Kathryn L. Hendron, Louis N. Awad, Thiago R. Teles Dos Santos, Vanessa L. De Araujo, et al. 2015. "A Soft Exosuit for Patients with Stroke: Feasibility Study with a Mobile off-Board Actuation Unit." *IEEE International Conference on Rehabilitation Robotics* 2015-Septe: 131–38. https://doi.org/10.1109/ICORR.2015.7281188.

Banala, Sai K., Seok Hun Kim, Sunil K. Agrawal, and John P. Scholz. 2009. "Robot Assisted Gait Training with Active Leg Exoskeleton (ALEX)." *IEEE Transactions on Neural Systems and Rehabilitation Engineering* 17 (1): 2–8. https://doi.org/10.1109/BIOROB.2008.4762885.

Barbareschi, Giulia, Rosie Richards, Matt Thornton, Tom Carlson, and Catherine Holloway. 2015. "Statically vs Dynamically Balanced Gait: Analysis of a Robotic Exoskeleton Compared with a Human." *Proceedings of the Annual International Conference of the IEEE Engineering in Medicine and Biology Society, EMBS* 2015-Novem: 6728–31. https://doi.org/10.1109/EMBC.2015.7319937.

Batchelor, Frances, Keith Hill, Shylie MacKintosh, and Catherine Said. 2010. "What Works in Falls Prevention after Stroke?: A Systematic Review and Meta-Analysis." *Stroke* 41 (8): 1715–22. https://doi.org/10.1161/STROKEAHA.109.570390.

Belda-Lois, Juan-Manuel, Silvia Mena-del Horno, Ignacio Bermejo-Bosch, Juan C Moreno, José L Pons, Dario Farina, Marco Iosa, et al. 2011. "Rehabilitation of Gait after Stroke: A Review towards a Top-down Approach." *Journal of NeuroEngineering and Rehabilitation* 8 (1): 66. https://doi.org/10.1186/1743-0003-8-66.

Bionics, Ekso. 2016. "Ekso Bionics - An Exoskeleton Suit or a Wearable Robot That Helps People Walk Again." 2016.

Bogousslavsky, J., G. Van Melle, and F. Regli. 1988. "The Lausanne Stroke Registry: Analysis of 1,000 Consecutive Patients with First Stroke." *Stroke: A Journal of Cerebral Circulation* 19 (9): 1083–92. https://doi.org/10.1161/01.STR.19.9.1083.

Bortole, Magdo, Anusha Venkatakrishnan, Fangshi Zhu, Juan C Moreno, Gerard E Francisco, Jose L Pons, and Jose L Contreras-Vidal. 2015. "The H2 Robotic Exoskeleton for Gait Rehabilitation after Stroke: Early Findings from a Clinical Study." *Journal of NeuroEngineering and Rehabilitation* 12 (1): 54. https://doi.org/10.1186/s12984-015-0048-y.

Chen, Gong, Chow Khuen Chan, Zhao Guo, and Haoyong Yu. 2013. "A Review of Lower Extremity Assistive Robotic Exoskeletons in Rehabilitation Therapy." *Critical Reviews in Biomedical Engineering* 41 (4–5): 343–63. https://doi.org/10.1615/CritRevBiomedEng.2014010453.

Danion, F, E Varraine, M Bonnard, and J Pailhous. 2003. "Stride Variability in Human Gait: The Effect of Stride Frequency and Stride Length" 18: 69–77. https://doi.org/10.1016/S0966-6362(03)00030-4.

Duschau-Wicke, Alexander, Joachim Von Zitzewitz, Andrea Caprez, Lars Lünenburger, and Robert Riener. 2010. "Path Control: A Method for Patient-Cooperative Robot-Aided Gait Rehabilitation." *IEEE Transactions on Neural Systems and Rehabilitation Engineering* 18 (1): 38–48. https://doi.org/10.1109/TNSRE.2009.2033061.

Esquenazi, Alberto, Mukul Talaty, Andrew Packel, and Michael Saulino. 2012. "The ReWalk Powered Exoskeleton to Restore Ambulatory Function to Individuals with Thoracic-Level Motor-Complete Spinal Cord Injury." *American Journal of Physical Medicine & Rehabilitation* 91 (11): 911–21. https://doi.org/10.1097/PHM.0b013e318269d9a3.

Farris, Ryan J, Hugo A Quintero, Clare Hartigan, and Michael Goldfarb. 2012. "A Preliminary Assessment of Mobility and Exertion in a Lower Limb Exoskeleton for Persons with Paraplegia" 22 (3): 53.

Fleischer, Christian, Andreas Wege, Konstantin Kondak, and Günter Hommel. 2006. "Application of EMG Signals for Controlling Exoskeleton Robots." *Biomedizinische Technik* 51 (5–6): 314–19. https://doi.org/10.1515/BMT.2006.063.

Forster, A, and J Young. 1995. "Incidence and Consequences of Falls Due to Stroke: A Systematic Inquiry." *BMJ (Clinical Research Ed.)* 311 (6997): 83–86. https://doi.org/10.1136/bmj.311.6997.83.

Garate, Virginia Ruiz, Andrea Parri, Tingfang Yan, Marko Munih, Raffaele Molino Lova, Nicola Vitiello, and Renaud Ronsse. 2017. "Experimental Validation of Motor Primitive-Based Control for Leg Exoskeletons during Continuous Multi-Locomotion Tasks." *Frontiers in Neurorobotics* 11 (MAR). https://doi.org/10.3389/fnbot.2017.00015.

Go, Alan S., Dariush Mozaffarian, Véronique L. Roger, Emelia J. Benjamin, Jarett D. Berry, Michael J. Blaha, Shifan Dai, et al. 2014. *Heart Disease and Stroke Statistics - 2014 Update: A Report from the American Heart Association*. *Circulation*. Vol. 129. https://doi.org/10.1161/01.cir.0000441139.02102.80.

Harris, Jocelyn E., Janice J. Eng, Daniel S. Marigold, Craig D. Tokuno, and Cheryl L. Louis. 2005. "Relationship of Balance and Mobility to Fall Incidence in People With Chronic Stroke." *Physical Therapy* 85 (2): 150–58.

Hartigan, Clare, Casey Kandilakis, Skyler Dalley, Mike Clausen, Edgar Wilson, Scott Morrison, Steven Etheridge, and Ryan Farris. 2015. "Mobility Outcomes Following Five Training Sessions with a Powered Exoskeleton." *Topics in Spinal Cord Injury Rehabilitation* 21 (2): 93–99. https://doi.org/10.1310/sci2102-93.

He, H., and K. Kiguchi. 2007. "A Study on EMG-Based Control of Exoskeleton Robots for Human Lower-Limb Motion Assist." *Proceedings of the IEEE/EMBS Region 8 International*

*Conference on Information Technology Applications in Biomedicine, ITAB*, 292–95. https://doi.org/10.1109/ITAB.2007.4407405.

Jorgensen, HS, H Nakayama, HO Raaschou, and TS Olsen. 1995. "Recovery of Walking Function in Stroke Patients: The Copenhagen Stroke Study." *Activities of Physical Medicine and Rehabilitation* 76: 27–32.

Kajita, S., F. Kanehiro, K. Kaneko, K. Fujiwara, K. Harada, K. Yokoi, and H. Hirukawa. 2014. "Biped Walking Pattern Generation by Using Preview Control of Zero-Moment Point." *2003 IEEE International Conference on Robotics and Automation (Cat. No.03CH37422)*, no. October 2003: 1620–26. https://doi.org/10.1109/ROBOT.2003.1241826.

Kawamoto, H., Suwoong Lee Suwoong Lee, S. Kanbe, and Y. Sankai. 2003. "Power Assist Method for HAL-3 Using EMG-Based Feedback Controller." *SMC'03 Conference Proceedings. 2003 IEEE International Conference on Systems, Man and Cybernetics. Conference Theme - System Security and Assurance (Cat. No.03CH37483)* 2: 1648–53. https://doi.org/10.1109/ICSMC.2003.1244649.

Kelly-Haynes, M., A. Beiser, C.S. Kase, A. Scaramucci, R.B. D'Agostino, and P.A. Wolf. 2003. "The Influence of Gender and Age on Disability Following Ischemic Stroke: The Framingham Study." *Journal of Stroke and Cerebrovascular Diseases* 12: 119–26.

Kozlowski, Allan, Thomas Bryce, and Marcel Dijkers. 2015. "Time and Effort Required by Persons with Spinal Cord Injury to Learn to Use a Powered Exoskeleton for Assisted Walking." *Topics in Spinal Cord Injury Rehabilitation* 21 (2): 110–21. https://doi.org/10.1310/sci2102-110.

la Fuente, Juan De, Thomas G. Sugar, and Sangram Redkar. 2017. "Nonlinear, Phase-Based Oscillator to Generate and Assist Periodic Motions." *Journal of Mechanisms and Robotics* 9 (2): 024502. https://doi.org/10.1115/1.4036023.

Lenzi, Tommaso, Maria Chiara Carrozza, and Sunil K. Agrawal. 2013. "Powered Hip Exoskeletons Can Reduce the User's Hip and Ankle Muscle Activations during Walking." *IEEE Transactions on Neural Systems and Rehabilitation Engineering* 21 (6): 938–48. https://doi.org/10.1109/TNSRE.2013.2248749.

Lerner, Zachary F., Diane L. Damiano, and Thomas C. Bulea. 2017. "A Lower-Extremity Exoskeleton Improves Knee Extension in Children with Crouch Gait from Cerebral Palsy." *Science Translational Medicine* 9 (404): 1–11. https://doi.org/10.1126/scitranslmed.aam9145.

Li, Perry Y, and Roberto Horowitz. 1999. "Passive Velocity Field Control of Mechanical Manipulators" 15 (4): 751–63.

Mackintosh, S F H, K Hill, K J Dodd, P Goldie, and E Culham. 2005. "Falls and Injury Prevention Should Be Part of Every Stroke Rehabilitation Plan." *Clin Rehabil* 19 (4): 441–51. http://eutils.ncbi.nlm.nih.gov/entrez/eutils/elink.fcgi?dbfrom=pubmed&id=15929514&retmode=ref&cmd=prlinks.

Marchal-Crespo, Laura, and David J Reinkensmeyer. 2009. "Review of Control Strategies for Robotic Movement Training after Neurologic Injury." *Journal of Neuroengineering and Rehabilitation* 6 (1): 20. https://doi.org/10.1186/1743-0003-6-20.

Martinez, A., B.E. Lawson, and M. Goldfarb. 2018. "A Controller for Guiding Leg Movement during Overground Walking with a Lower Limb Exoskeleton." *Transactions on Robotics* 34 (1): 183–93.

Martinez, Andres, Brian Lawson, Christina Durrough, and Michael Goldfarb. 2018. "A Velocity-Field-Based Controller for Assisting Leg Movement During Walking With a Bilateral Hip and Knee Lower Limb Exoskeleton." *IEEE Transactions on Robotics*, 1–10. https://doi.org/10.1109/TRO.2018.2883819.

Mehrholz, J., B. Elsner, C. Werner, J. Kugler, and M. Pohl. 2013. "Electromechanical-Assisted Training for Walking After Stroke: Updated Evidence." *Stroke* 44 (10): e127–28. https://doi.org/10.1161/STROKEAHA.113.003061.

Meng, Wei, Quan Liu, Zude Zhou, Qingsong Ai, Bo Sheng, and Shengquan Shane Xie. 2015. "Recent Development of Mechanisms and Control Strategies for Robot-Assisted Lower Limb Rehabilitation." *Mechatronics* 31: 132–45. https://doi.org/10.1016/j.mechatronics.2015.04.005.

Michael, Kathleen M., Jerilyn K. Allen, and Richard F. MacKo. 2005. "Reduced Ambulatory Activity after Stroke: The Role of Balance, Gait, and Cardiovascular Fitness." *Archives of Physical Medicine and Rehabilitation* 86 (8): 1552–56. https://doi.org/10.1016/j.apmr.2004.12.026.

Murray, Spencer A., Kevin H. Ha, Clare Hartigan, and Michael Goldfarb. 2015. "An Assistive Control Approach for a Lower-Limb Exoskeleton to Facilitate Recovery of Walking Following Stroke." *IEEE Transactions on Neural Systems and Rehabilitation Engineering* 23 (3): 441–49. https://doi.org/10.1109/TNSRE.2014.2346193.

Neuhaus, Peter D., Jerryll H. Noorden, Travis J. Craig, Tecalote Torres, Justin Kirschbaum, and Jerry E. Pratt. 2011. "Design and Evaluation of Mina: A Robotic Orthosis for Paraplegics." *IEEE International Conference on Rehabilitation Robotics*. https://doi.org/10.1109/ICORR.2011.5975468.

Perry, Jacquelin, and Judith M. Burnfield. 2010. *Gait Analysis: Normal and Pathological Function*. 2nd ed. New Jersey: SLACK Inc.

Pouwels, Sander, Arief Lalmohamed, Bert Leufkens, Anthonius De Boer, Cyrus Cooper, Tjeerd Van Staa, and Frank De Vries. 2009. "Risk of Hip/Femur Fracture after Stroke: A Population-Based Case-Control Study." *Stroke* 40 (10): 3281–85. https://doi.org/10.1161/STROKEAHA.109.554055.

Quinlivan, B. T., S. Lee, P. Malcolm, D. M. Rossi, M. Grimmer, C. Siviy, N. Karavas, et al. 2017. "Assistance Magnitude versus Metabolic Cost Reductions for a Tethered Multiarticular Soft Exosuit." *Science Robotics* 2 (2): eaah4416. https://doi.org/10.1126/scirobotics.aah4416.

Quintero, Hugo A, Ryan J Farris, and Michael Goldfarb. 2012. "A Method for the Autonomous Control of Lower Limb Exoskeletons for Persons with Paraplegia." *Journal of Medical Devices* 6 (4): 041003. https://doi.org/10.1115/1.4007181.

Ronsse, Renaud, Tommaso Lenzi, Nicola Vitiello, Bram Koopman, Edwin Van Asseldonk, Stefano Marco Maria De Rossi, Jesse Van Den Kieboom, Herman Van Der Kooij, Maria Chiara

Carrozza, and Auke Jan Ijspeert. 2011. “Oscillator-Based Assistance of Cyclical Movements: Model-Based and Model-Free Approaches.” *Medical and Biological Engineering and Computing* 49 (10): 1173–85. https://doi.org/10.1007/s11517-011-0816-1.

Sawicki, Gregory S., and Daniel P. Ferris. 2009. “A Pneumatically Powered Knee-Ankle-Foot Orthosis (KAFO) with Myoelectric Activation and Inhibition.” *Journal of NeuroEngineering and Rehabilitation* 6 (1): 1–16. https://doi.org/10.1186/1743-0003-6-23.

Sugar, Thomas G., Andrew Bates, Matthew Holgate, Jason Kerestes, Marc Mignolet, Philip New, Ragesh K. Ramachandran, Sangram Redkar, and Chase Wheeler. 2015. “Limit Cycles to Enhance Human Performance Based on Phase Oscillators.” *Journal of Mechanisms and Robotics* 7 (1): 011001. https://doi.org/10.1115/1.4029336.

Suzuki, Kenta, Gouji Mito, Hiroaki Kawamoto, Yasuhisa Hasegawa, and Yoshiyuki Sankai. 2007. “Intention-Based Walking Support for Paraplegia Patients with Robot Suit HAL.” *Advanced Robotics* 21 (12): 1441–69. https://doi.org/10.1163/156855307781746061.

Vallery, Heike, Alexander Duschau-Wicke, and Robert Riener. 2009. “Generalized Elasticities Improve Patient-Cooperative Control of Rehabilitation Robots.” *2009 IEEE International Conference on Rehabilitation Robotics, ICORR 2009*, no. June: 535–41. https://doi.org/10.1109/ICORR.2009.5209595.

Vallery, Heike, Jan Frederik Veneman, Edwin Van Asseldonk, Ralf Ekkelenkamp, Martin Buss, and Herman Van Der Kooij. 2008. “Compliant Actuation of Rehabilitation Robotics.” *IEEE Robotics & Automation Magazine* 15 (3): 60–69.

Wang, Shiqian, Letian Wang, Cory Meijneke, Edwin Van Asseldonk, Thomas Hoellinger, Guy Cheron, Yuri Ivanenko, et al. 2014. “Design and Evaluation of the Mindwalker Exoskeleton.” *IEEE Transactions on Neural Systems and Rehabilitation Engineering : A Publication of the IEEE Engineering in Medicine and Biology Society* 4320 (c): 277–86. https://doi.org/10.1109/TNSRE.2014.2365697.

Wang, Shiqian, Letian Wang, Cory Meijneke, Edwin Van Asseldonk, Thomas Hoellinger, Guy Cheron, Yuri Ivanenko, et al. 2015. “Design and Control of the MINDWALKER Exoskeleton.” *IEEE Transactions on Neural Systems and Rehabilitation Engineering* 23 (2): 277–86. https://doi.org/10.1109/TNSRE.2014.2365697.

Wang, Yang, and Manoj Srinivasan. 2014. “Stepping in the Direction of the Fall: The next Foot Placement Can Be Predicted from Current Upper Body State in Steady-State Walking.” *Biology Letters* 10 (9): 1–9. https://doi.org/10.1098/rsbl.2014.0405.

Ward, Jeffrey, Thomas Sugar, Alexander Boehler, John Standeven, and Jack R. Engsberg. 2012. “Stroke Survivors’ Gait Adaptations to a Powered Ankle Foot Orthosis.” *Advanced Robotics* 25 (15): 1879–1901. https://doi.org/10.1163/016918611X588907.Stroke.

Weerdesteyn, Vivian, Mark de Niet, Hanneke van Duijnohoven, and Alexander Geurts. 2008. “Falls in Individuals with Stroke.” *Journal of Rehabilitation Research and Development* 45 (8): 1195–1213.

Winter, David A. 1991. *Biomechanics and Motor Control of Human Gait: Normal, Elderly and Pathological*.

Yan, Tingfang, Marco Cempini, Calogero Maria Oddo, and Nicola Vitiello. 2015. "Review of Assistive Strategies in Powered Lower-Limb Orthoses and Exoskeletons." *Robotics and Autonomous Systems* 64: 120–36. https://doi.org/10.1016/j.robot.2014.09.032.

Yin, Yue H., Yuan J. Fan, and Li D. Xu. 2012. "EMG and EPP-Integrated Human-Machine Interface between the Paralyzed and Rehabilitation Exoskeleton." *IEEE Transactions on Information Technology in Biomedicine* 16 (4): 542–49. https://doi.org/10.1109/TITB.2011.2178034.

Young, A.J., and D.P. Ferris. 2017. "State-of-the-Art and Future Directions for Robotic Lower Limb Robotic Exoskeletons." *IEEE Transactions on Neural Systems and Rehabilitation Engineering* 25 (2): 171–82. https://doi.org/10.1109/TNSRE.2016.2521160.

Young, Aaron J., Hannah Gannon, and Daniel P. Ferris. 2017. "A Biomechanical Comparison of Proportional Electromyography Control to Biological Torque Control Using a Powered Hip Exoskeleton." *Frontiers in Bioengineering and Biotechnology* 5 (June). https://doi.org/10.3389/fbioe.2017.00037.